A Cysteine Scan of the Inner Vestibule of Cyclic Nucleotide–gated Channels Reveals Architecture and Rearrangement of the Pore

Galen E. Flynn[1] and William N. Zagotta[1,2]

[1]Department of Physiology and Biophysics, [2]Howard Hughes Medical Institute, University of Washington, Seattle, WA 98195

ABSTRACT Cyclic nucleotide–gated (CNG) channels belong to the P-loop–containing family of ion channels that also includes KcsA, MthK, and Shaker channels. In this study, we investigated the structure and rearrangement of the CNGA1 channel pore using cysteine mutations and cysteine-specific modification. We constructed 16 mutant channels, each one containing a cysteine mutation at one of the positions between 384 and 399 in the S6 region of the pore. By measuring currents activated by saturating concentrations of the full agonist cGMP and the partial agonists cIMP and cAMP, we show that mutating S6 residues to cysteine caused both favorable and unfavorable changes in the free energy of channel opening. The time course of cysteine modification with 2-aminoethylmethane thiosulfonate hydrochloride (MTSEA) was complex. For many positions we observed decreases in current activated by cGMP and concomitant increases in current activated by cIMP and cAMP. A model where modification affected both gating and permeation successfully reproduced the complex time course of modification for most of the mutant channels. From the model fits to the time course of modification for each mutant channel, we quantified the following: (a) the bimolecular rate constant of modification in the open state, (b) the change in conductance, and (c) the change in the free energy of channel opening for modification of each cysteine. At many S6 cysteines, modification by MTSEA caused a decrease in conductance and a favorable change in the free energy of channel opening. Our results are interpreted within the structural framework of the known structures of KcsA and MthK. We conclude that: (a) MTSEA modification affects both gating and permeation, (b) the open configuration of the pore of CNGA1 channels is consistent with the structure of MthK, and (c) the modification of S6 residues disrupts the helical packing of the closed channel, making it easier for channels to open.

KEY WORDS: cyclic nucleotide–gated channel • cysteine • protein structure • ion channel gating

INTRODUCTION

Ion channels are integral membrane proteins that regulate ion fluxes across membranes and thereby control membrane excitability. To regulate ion fluxes, channels undergo conformational changes that close and open their ion-permeable pore, a process referred to as gating. Gating is in turn allosterically regulated by changes in membrane voltage or binding of agonists. CNG channels are a prototypic ion channel gated by the binding of agonists. CNG channels are closed or opened in response to changes in the cytoplasmic concentrations of cyclic nucleotides (Yau and Baylor, 1989). Cyclic nucleotides bind directly to a cytoplasmic binding domain on the channel which, in turn, is allosterically coupled to the opening of the pore in these channels (Fesenko et al., 1985; Nakamura and Gold, 1987). When opened, CNG channels allow an influx of cations that depolarizes the plasma membrane. This is the regulatory mechanism that underlies the electrical response of photoreceptors and olfactory receptors to sensory stimuli (Burns and Baylor, 2001; Zufall and Munger, 2001). In addition, these channels are expressed in a number of other tissues where their function is less well characterized (for review see Kraus-Friedmann, 2000).

The first CNG channel cloned (CNGA1) was isolated from bovine rod photoreceptors (Kaupp et al., 1989). It shares sequence similarity with the voltage-gated ion channel superfamily, although CNG channels are only weakly voltage dependent (Yau and Baylor, 1989; Jan and Jan, 1990). Like voltage-gated potassium channels, CNG channels are composed of four subunits (Liu et al., 1996; Varnum and Zagotta, 1996). Each subunit contains cytoplasmic amino and carboxy termini, six transmembrane segments (S1–S6), a charged S4 region, and a P-loop between S5 and S6 (Kaupp et al., 1989; Molday et al., 1991; Wohlfart et al., 1992; Henn et al., 1995; Liu et al., 1996). Within each carboxy-terminal region, CNG channels have a cyclic nucleotide–binding domain (CNBD)* that exhibits sequence similarity to other cyclic nucleotide-binding proteins (for review see Shabb and Corbin, 1992). Direct binding of cyclic nucleotides to this specialized domain leads to opening of the CNG channel pore.

Address correspondence to William N. Zagotta, Department of Physiology and Biophysics, Box 357290, University of Washington, Seattle, WA 98195-7290. Fax: (206) 543-0934; E-mail: Zagotta@u.washington.edu

*Abbreviations used in this paper: CNBD, cyclic nucleotide–binding domain; IRK, inward rectifier; MTSEA, 2-aminoethylmethane thiosulfonate hydrochloride; MTSET, 2-trimethylammonioethylmethane thiosulfonate hydrochloride; TPeA, tetrapentylammonium.

J. Gen. Physiol. © The Rockefeller University Press • 0022-1295/2003/06/563/20 $8.00
Volume 121 June 2003 563–582
http://www.jgp.org/cgi/doi/10.1085/jgp.200308819

CNG channel pores are thought to be structurally similar to that of other P-loop–containing ion channels (Goulding et al., 1993; Sun et al., 1996; Becchetti et al., 1999; Becchetti and Roncaglia, 2000; Liu and Siegelbaum, 2000; Flynn and Zagotta, 2001) (Fig. 1). The basic architectural plan of an ion channel pore was revealed by the crystal structure of KcsA, a bacterial potassium channel from *Streptomyces lividans* (Doyle et al., 1998). KcsA is a tetramer of identical subunits arranged with fourfold symmetry about a centrally located pore. A single KcsA subunit has two membrane-spanning helices, the outer and inner helices, and a reentrant P-loop. Each subunit of the tetramer contributes its P-loop to the formation of the pore. The P-loop starts from the extracellular side and enters the membrane as an α-helix (pore helix) that then exits back extracellularly as an uncoiled strand. Within this strand, permeant cations are coordinated by the backbone carbonyl oxygens of the amino acids TVGYG, which are recognized as the signature sequence of K^+-selective channels (Heginbotham et al., 1994). Intracellular to the selectivity filter is a large (~10 Å in diameter; Doyle et al., 1998) water-filled vestibule. In the center of this cavity another permeant cation is stabilized through both electrostatic interactions with the pore helices and water molecules that hydrate the cation (Doyle et al., 1998; Roux and MacKinnon, 1999; Zhou et al., 2001). The membrane-spanning inner helices line the vestibule of the channel and cross the membrane at an angle to form a helix bundle on the intracellular side (Doyle et al., 1998). The helix bundle defines the intracellular entrance to the pore of KcsA that is thought to be in the closed state. To open the pore, a conformation change is thought to occur in the inner helix. An open conformation was revealed by the crystal structure of another ion channel, MthK (Jiang et al., 2002a,b). MthK is structurally similar to KcsA in the P-loop but exhibits a different conformation of the inner helix. In MthK, the inner helix contains a "gating hinge" near the top of the vestibule that bends this helix by 30°, creating a 12 Å opening on the intracellular side of the pore compared with the 4 Å opening of the helix bundle of KcsA. Amino acid conservation among a wide range of P-loop–containing channels suggests that the KcsA and MthK structures may serve as general models for the closed and open state conformations for this entire family of ion channels (Jiang et al., 2002b).

Using site-specific cysteine substitution, we have suggested previously that the cytoplasmic opening of the CNG channel pore is narrow when channels are closed and widens when channels open (Flynn and Zagotta, 2001). Substituting a cysteine (S399C, Fig. 1) at the cytoplasmic end of the S6 (the putative inner helix) in a cysteine-free variant of CNGA1 channels promotes channel closure through the spontaneous formation of an intersubunit disulfide bond. Since disulfide bonds are formed between cysteine residues ~10 Å apart (Falke et al., 1988; Careaga and Falke, 1992), this result is consistent with a narrow cytoplasmic opening and the occurrence of a helix bundle similar to the one in KcsA. Furthermore, this disulfide bond forms much faster when channels are closed than when channels are open, suggesting a conformational change in the helix bundle of CNGA1 channels that widens the intracellular entrance of the pore. A widening of the intracellular entrance is necessary to explain the voltage-dependent block by large molecules such as tetrapentylammonium (TPeA) ions that enter the inner vestibule and block CNGA1 channels (Stotz and Haynes, 1996). Although the helix bundle defines a narrow cytoplasmic opening to the pore when channels are closed, its permeability to small cationic cysteine modifiers, such as Ag^+ and 2-aminoethylmethane thiosulfonate hydrochloride (MTSEA), is state independent. These results are consistent with a model where the intracellular entrance of the pore of CNG channels widens during opening but is not itself the gate that controls permeation through the membrane (Flynn and Zagotta, 2001).

Several investigations have shown that the gating process in CNG channels is sensitive to perturbations of the pore structure (Sun et al., 1996; Bucossi et al., 1997; Fodor et al., 1997; Becchetti et al., 1999; Liu and Siegelbaum, 2000; Flynn et al., 2001). The sensitivity of the gating mechanism to mutational and biochemical perturbations provides useful information about the energetic and structural changes that occur during the final closed-to-open transition. In this study, we focused on the conformational change in the pore that is initiated by cyclic nucleotide binding to the CNBD. We replaced each residue in the S6 helix from 384 to 399 with cysteine (Fig. 1) and quantified changes in function in response to mutational and biochemical perturbations in the pore.

MATERIALS AND METHODS

Molecular Biology and Channel Expression

We introduced reporter cysteines into the S6 region of $CNGA1_{cys\text{-}free}$ channels. $CNGA1_{cys\text{-}free}$ is a cysteine-free variant of CNGA1 (Kaupp et al., 1989) with the mutations C35A, C169S, C186S, C314S, C481F, C505V, and C573V that remove all endogenous cysteine residues from the channel (Matulef et al., 1999). In addition, $CNGA1_{cys\text{-}free}$ had a K2E mutation to create an Nco1 site and a FLAG™ epitope (DYKDDDDK) that replaced the last five residues at the carboxy terminus. This construct was also used as the B protomer in tandem dimer experiments (see below). The cyclic nucleotide specificity of $CNGA1_{cys\text{-}free}$ channels was the same as CNGA1 channels but the efficacies and apparent affinities for each cyclic nucleotide were higher primarily due to the C481F mutation (Matulef et al., 1999). For these experiments, PCR methods were used to replace a single codon in the cDNA

encoding $CNGA1_{cys\text{-}free}$ with the codon for cysteine. Each mutation was confirmed by DNA sequencing (PE Applied Biosystems, Inc.). 16 mutant channels were generated in total, one for each amino acid position between 384 and 399 in the CNGA1 channel protein. Nhe1-linearized cDNAs were transcribed in vitro to cRNAs using the T7 Message Machine kit (Ambion). For protein expression, *Xenopus* oocytes were injected with 40 nl of cRNA (~1 μg/μl) and stored at 18°C for 4–10 d in a solution containing (in mM) 96 NaCl, 2 KCl, 1.8 $CaCl_2$, 1 $MgCl_2$, 5 HEPES at pH 7.6 (Zagotta et al., 1989). All chemicals were purchased from Sigma-Aldrich unless indicated otherwise.

For tandem dimers experiments, the coding sequences of two subunits (A and B protomers) were joined by a linker region in a single open reading frame and expressed in oocytes to form channels containing two A protomers and two B protomers (see previously described methods in Gordon and Zagotta, 1995b; Varnum et al., 1995). All A protomers included a COOH-terminal 21 amino acid peptide linker (Q_8IEGRQ_8A) followed by an Nco1 restriction site. All B protomers contained an Nco1 restriction site at the initial methionine. The entire coding sequence for the A protomer plus linker was excised and inserted into a pGEMHE vector containing the B protomer sequence. For heterodimeric S399C channel expression, the construct encoded a $CNGA1_{cys\text{-}free}$ subunit (A protomer) connected to a S399C subunit (B protomer) separated by the peptide linker sequence. For homodimeric S399C channel expression, both A and B protomers contained the S399C mutation. DNA and mRNA were analyzed by agarose gel electrophoresis to confirm the presence of a single dimer-size construct before injection of mRNA into oocytes.

Electrophysiology

Electrophysiological data were collected from excised, inside-out patches of membrane from defolliculated oocytes using the patch-clamp technique (Hamill et al., 1981). All recordings were made at room temperature (20–22°C). Recording electrodes were fashioned from borosilicate glass (VWR International) that was polished to resistances of 0.2–1.0 mΩ when filled with recording solutions. Inside each glass electrode, a 0.6% agar, 3 M KCl bridge was fit over the Ag-AgCl electrode wire to increase the stability of recordings. Electrodes were filled with a solution (extracellular) that contained (in mM): 130 NaCl, 3 HEPES, 0.5 niflumic acid, and 0.2 EDTA at pH 7.2. Niflumic acid was added to inhibit calcium-activated chloride currents endogenous to oocytes (White and Aylwin, 1990). The bath solution (intracellular) contained (in mM): 130 NaCl, 3 HEPES, and 0.2 EDTA at pH 7.2. To activate $CNGA1_{cys\text{-}free}$ and cysteine mutant channels, saturating concentrations of cyclic nucleotides (2.5 mM cGMP, 16 mM cIMP, 16 mM cAMP) were applied to the intracellular surface of each patch using a rapid solution changer (RSC-100; Bio-logic). A three-step voltage protocol was applied to the patches that consisted of three 100 ms pulses to −60, +60, and −60 mV from a holding potential of 0 mV. Ionic currents were amplified and low-pass filtered at 2 kHz by an AxoPatch 200A (Axon Instruments, Inc.). The currents were digitized at 10 kHz using an ITC-16 board (Instrutech Corp.) interfaced to a Pentium 3 computer (Dell Computer Corp.) running Pulse software (HEKA Electronics, Inc.) and stored in files for offline analysis using Igro software (Wavemetrics, Inc.) or Excel software (Microsoft).

For all the experiments in this study, currents in the absence of cyclic nucleotide have been subtracted so that the data shown are only of currents through cyclic nucleotide-activated channels. After patch excision, we observed a slow increase in current through $CNGA1_{cys\text{-}free}$ channels that required 20–25 min to stabilize. This increase in current has been attributed to dephosphorylation of the channel (Molokanova et al., 1999; Kramer and Molokanova, 2001). Most of our experiments were performed 30 min after patch excision to accommodate the increase in current that occurs after patch excision. A388C and S399C channels exhibited a spontaneous decline in current amplitude following patch excision. As a consequence, these mutants were examined immediately following patch excision and were analyzed relative to $CNGA1_{cys\text{-}free}$ channels immediately after patch excision.

Cysteine Modification

We applied MTSEA (2-aminoethylmethane thiosulfonate hydrochloride) to the intracellular side of $CNGA1_{cys\text{-}free}$ channels and each of the 16 mutant channels. Stock solutions of 100 mM MTSEA (Toronto Research Chemical) were made in water and stored at −80°C until just before application. MTSEA was diluted to the indicated concentration in the intracellular solution containing 2.5 mM cGMP. To study the kinetic effects of cysteine modification, mutant channels were partially modified by a brief exposure (~10 s) to MTSEA applied to the intracellular side. Patches were then washed free of modifier and currents were activated by saturating concentrations of cGMP, cIMP, and cAMP. Measurements of cyclic nucleotide–activated currents were made at 2–3 ms after the initiation of +60- and −60-mV pulses in order to limit contamination by ion accumulation and depletion effects (Zimmerman et al., 1988). Currents in the absence of nucleotides were also measured. Patches were then reexposed to MTSEA and the cycle of solutions continued until no further changes in current were observed (see Fig. 6).

Determination of Mutational Effects on Gating

The effects on the free energy difference between the closed and open states caused by the cysteine mutation were quantified for each mutant channel. We assumed that the opening transition for a channel fully bound by agonist can be described by a simple closed-to-open equilibrium with equilibrium constant (L). The approach used actually measures resting-to-activated states but for simplicity will be referred to as closed and open states respectively. The behavior of the different agonists can be explained by L values specific for each agonist (L_{cGMP}, L_{cIMP}, and L_{cAMP}; Varnum et al., 1995; Varnum and Zagotta, 1996; Sunderman and Zagotta, 1999). The L values specific to each agonist were determined for each mutant channel assuming that the ratios L_{cIMP}/L_{cGMP} and L_{cAMP}/L_{cGMP} were fixed to 0.05 and 0.001, respectively, and were the same for all mutations. Currents activated by all three cyclic nucleotides were measured at both +60 and −60 mV. Analysis of the $CNGA1_{cys\text{-}free}$ channels at both +60 and −60 mV indicated that the voltage dependence of L was very weak (e-fold per 460 ± 59 mV; $n = 7$). Therefore, we assumed that the L values were voltage independent. The maximum current when all channels are open (I_{max}) and L_{cGMP} was determined by minimizing the least squares difference between currents observed and currents calculated (cal) according to the following equations:

$$I_{cGMP,cal} = I_{\max}\left(\frac{L_{cGMP}}{1 + L_{cGMP}}\right)$$

$$I_{cIMP,cal} = I_{\max}\left[\frac{\left(\frac{L_{cIMP}}{L_{cGMP}}\right)L_{cGMP}}{1 + \left(\frac{L_{cIMP}}{L_{cGMP}}\right)L_{cGMP}}\right]$$

$$I_{cAMP,cal} = I_{\max}\left[\frac{\left(\frac{L_{cAMP}}{L_{cGMP}}\right)L_{cGMP}}{1 + \left(\frac{L_{cAMP}}{L_{cGMP}}\right)L_{cGMP}}\right].$$

From these L values, the free energy difference between closed and open states was determined according to the relationship $\Delta G_{L,cNMP} = -RT\ln(L_{cNMP})$, where R is the ideal gas constant and T is temperature in Kelvin. All fits converged and the statistical results for each channel are shown as box plots or mean ± SEM as indicated.

Model for Determining the Modification Effects on Gating and Permeation

The rate of modification and the effects on gating and permeation were quantified by fitting a model to the time course of modification for each of the 16 cysteine mutant channels (see Fig. 8). Currents activated by all three cyclic nucleotides were measured at both +60 and −60 mV and plotted as a function of the cumulative exposure time in MTSEA. These time courses were fit with the equation below:

$$I(t) = I_{max} \sum_{N=0}^{4} \binom{4}{N} P^N (1-P)^{4-N} (Ln^N / [1 + Ln^N])(1 - Ng).$$

I(t) represents either I_{cGMP}, I_{cIMP}, or I_{cAMP} as a function of cumulative exposure time to MTSEA. L represents L_{cGMP}, L_{cIMP}, or L_{cAMP} as described above and was assumed to be voltage independent. I_{max} represents either $I_{max,+60\ mV}$ or $I_{max,-60\ mV}$ as described above. P is the probability that a subunit is modified and follows an exponential time course ($P = 1 - e^{(-t/\tau)}$). The free parameters in this model represent the fractional change per subunit in the equilibrium constant of the opening transition (n), the fractional change in conductance per subunit (g), and time constant of modification per subunit (τ). All fits converged and the statistical results for each channel are shown as box plots or mean ± SEM as indicated.

Details for Analysis of Specific Mutants

A388C and S399C channels exhibited spontaneous declines in current amplitude after patch excision. In A388C channels, the decline in current was the result of desensitization since much of the current was recoverable after channels were closed for a period of time. However, a slow irreversible decline was also observed. The decline in S399C was attributed to the spontaneous formation of a disulfide bond (Flynn and Zagotta, 2001). Therefore, experiments on A388C and S399C channel were performed immediately after patch excision. Because we were unable to wait for the dephosphorylation of these two channels to reach steady-state before applying MTSEA, we analyzed these two channels relative to $CNGA1_{cys\text{-}free}$ channels where experiments were performed immediately after patch excision.

Our analysis of the energetic effects on channel opening caused by cysteine mutations depends significantly on at least two cyclic nucleotides producing measurable currents with distinguishable amplitudes. G395C channels have such an unfavorable opening transition that the cGMP-activated currents were small and cIMP- and cAMP-activated currents were indiscernible from leak currents. However, MTSEA modification produced a dramatic increase in the currents activated by all three cyclic nucleotides and a pronounced inward rectification in G395C channels (see Fig. 12). Therefore, we used the modified channel to determined the maximum current ($I_{max,-60\ mV}$) and the free energy of the opening transition ($\Delta G_{L,cGMP,MTSEA}$) at −60 mV after MTSEA modification. Based on the ratio of current activated at −60 mV by cGMP before MTSEA modification relative to $I_{max,-60\ mV}$ determined after modification, we calculated $\Delta G_{L,cGMP}$ for G395C channels. In addition, for G392C channels after partial modification, currents activated by the three cyclic nucleotides were indistinguishable, and we were therefore unable to determine the change in the equilibrium constant caused by modification (n).

One of the limitations of the model is its inability to determine the number of subunits that are modified when the currents activated by all the cyclic nucleotides decay to zero with modification. This was the case for V384C, F387C, A388C, V391C, and G392C channels (see V384C Fig. 6). For these mutant channels we constrained the change in conductance (g) to ≤ 0.25.

The model describes effects of modification on gating and permeation and assumes that no change occurs in the cysteine residue other than MTSEA modification. However, we observed in G395C channels a behavior consistent with thiol-disulfide exchange when modification was slow relative to disulfide bond formation (see Fig. 15) (Creighton, 1984). To determine the effects of MTSEA modification on gating and permeation in G395C channels, currents activated by the three cyclic nucleotides were measured before and after rapid modification by 2 mM MTSEA. The free energy of the opening transition at −60 mV after modification ($\Delta G_{L,cGMP,MTSEA}$) was determined by simultaneously fit-

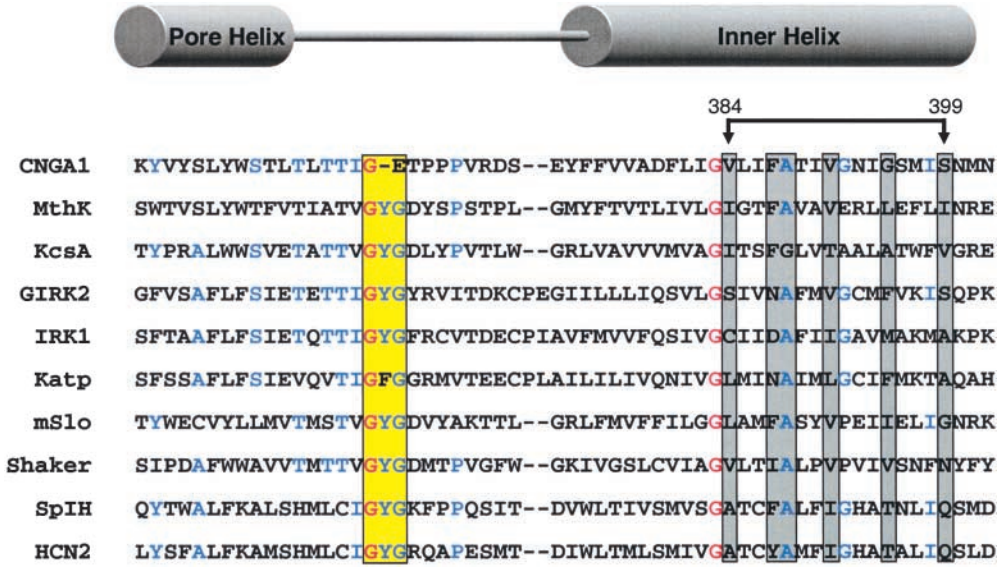

FIGURE 1. Sequence alignment of the pore helix, selectivity filter, and inner helix for several channels of the P-loop–containing family. Amino acids in blue are conserved among several channels and amino acids in red are identical for all channels. The selectivity filter is highlighted by a yellow box, and inner helix residues that line the pore of KcsA are highlighted in gray boxes. The inner helix region between arrows shows residues that were substituted with cysteine in this study.

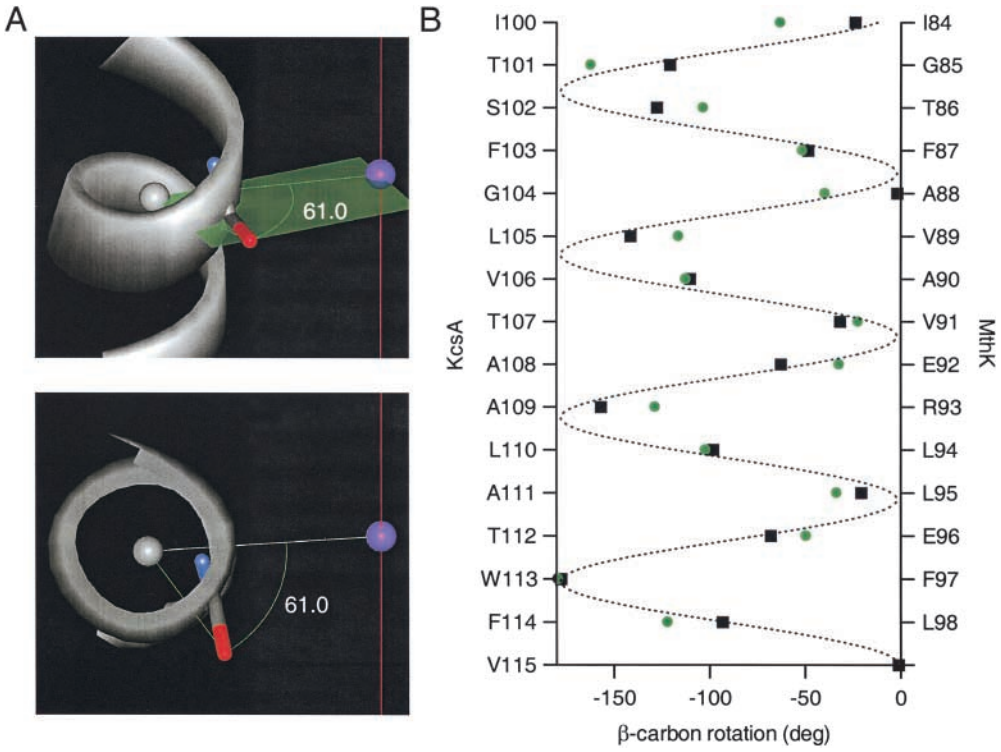

FIGURE 2. Angle of rotation away from the central pore axis of KcsA. (A) Side (top) and axial (bottom) view of the inner helix (ribbon) of KcsA in relation to the pore axis (red line, purple sphere). The pore axis (purple sphere) and the inner helix axis (gray sphere) are connected by a line (white) representing a 0° rotation angle. The β carbon of alanine 108 in KcsA is shown in red along with the angle of rotation away from the pore axis (61°). (B) Beta carbon angles of KcsA residues 100–115 (squares) or MthK residues 84–98 (circles). Dashed line is a sine function fit to the data.

ting the amplitudes of cyclic nucleotide–activated currents after rapid MTSEA exposure using the method of least squares. The energetic effects per subunit of G395C modification were calculated from the relationship $\Delta\Delta G_{L,MTSEA} = (\Delta G_{LcGMP,MTSEA} - \Delta G_{L,cGMP})/4$ where $\Delta G_{L,cGMP}$ was determine using the methods described above. Also, we calculated the change in conductance per subunit (g) as the ratio between the amplitude of the cGMP-activated current measured from modified G395C channels and the $I_{max,+60\ mV}$, predicted from L_{cGMP} (see above), i.e., $g = [1 - (I_{cGMP,MTSEA}/I_{max,+60\ mV})]/4$. The bimolecular rate constant of modification was not determined.

During the time course of MTSEA modification of S399C channels, the fractional activation by cIMP initially decreased and then increased, and the fractional activation by cAMP increased with a delay (see Fig. 16). This effect of modification on gating was different from the monotonic time course of the fractional activations of other S6 mutants in response to modification. Therefore, $\Delta\Delta G_{L,MTSEA}$ for S399C channels could not be determined.

Mapping Function to Known Structures

Structural hypotheses were tested by mapping the parameters from the kinetic model onto two homology models of the CNGA1 S6 region made using the software Swiss-PDB viewer in conjunction with the Swiss-Model protein modeling server (Guex and Peitsch, 1997). The closed state of the CNGA1 pore region was modeled after KcsA (Doyle et al., 1998) while the open state was modeled after MthK (Jiang et al., 2002b). The angle of rotation made by each β carbon in the inner helix of the KcsA and the MthK structures was measured relative to the central pore axis. A rotation angle was defined as the angle made by two lines when projected on a plane perpendicular to the pore axis; one connecting the β carbon to the longitudinal axis of the inner helix and the second connecting the central pore axis to the longitudinal axis of the inner helix (Fig. 2 A; A108 shown). The second line represents an angle of 0° rotation. Angles of β carbon rotation were measured for those KcsA and MthK residues that aligned with CNGA1 residues 384–399 (Fig. 1). The angles of rotation were plotted versus amino acid number for both KcsA and MthK and a clear sinusoidal pattern of an α helix was evident (Fig. 2 B). All structural models were analyzed and displayed using ViewerPro software (Accelrys).

RESULTS

Cysteine Replacement of S6 Residues Alters Gating

In this study, we substituted a cysteine for each of the S6 residues between 384 and 399 of a cysteine-free CNGA1 variant ($CNGA1_{cys\text{-}free}$) and expressed these mutant channels in *Xenopus* oocytes. Using the patch-clamp technique, we recorded currents from inside-out patches in response to a three-step voltage protocol consisting of three 100-ms pulses to −60, 60, and −60 mV from a holding potential of 0 mV (Fig. 3, inset). Channels were activated with saturating concentrations of cyclic nucleotides (2.5 mM cGMP, green; 16 mM cIMP, blue; 16 mM cAMP, red; see examples in Fig. 3) applied to the intracellular surface of these patches. For all the experiments in this study, currents in the absence of cyclic nucleotide have been subtracted so that the data shown are only of currents through CNG channels.

In $CNGA1_{cys\text{-}free}$ channels, cIMP activated only a fraction of the current activated by cGMP (I_{cIMP}/I_{cGMP} = 0.81 ± 0.02; n = 7, Fig. 3 A, blue trace). A smaller fraction of current was activated in response to cAMP

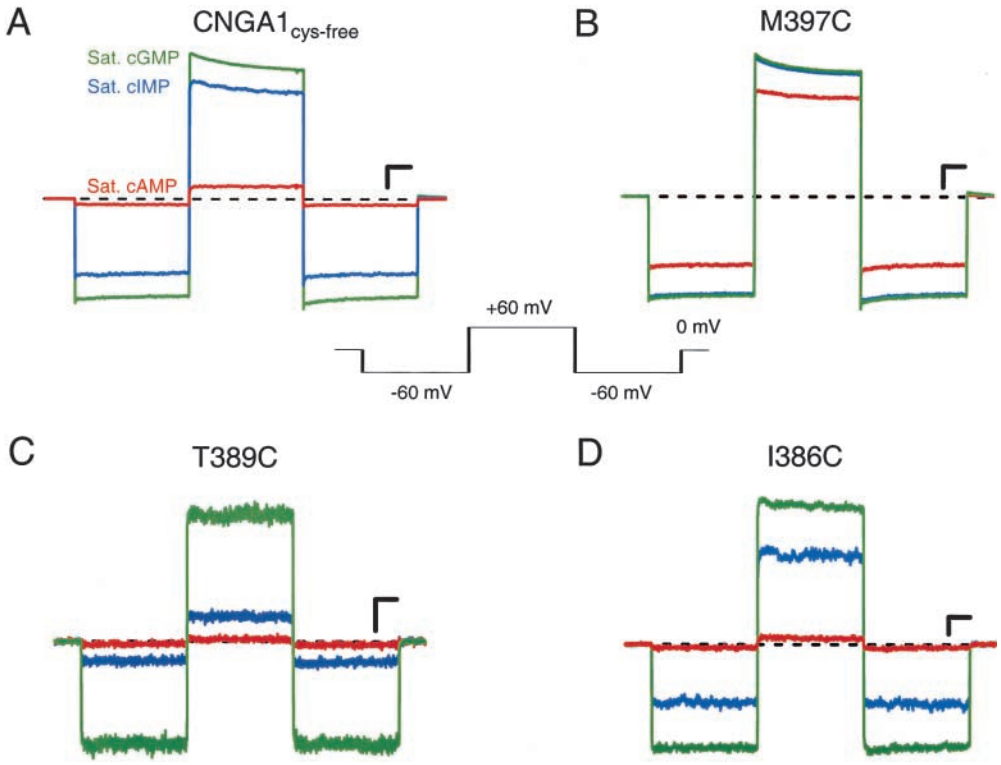

FIGURE 3. Effects of cysteine substitution on cyclic nucleotide-activated currents in $CNGA1_{cys\text{-}free}$ and three mutant channels. Representative currents traces from inside-out patches excised from *Xenopus* oocytes expressing either $CNGA1_{cys\text{-}free}$ or one of three mutant channels. Channels were activated by saturating concentrations of cGMP (green; 2.5 mM), cIMP (blue; 16 mM), cAMP (red; 16 mM). Currents were recorded in response to a three-step voltage protocol; 100-ms voltage steps to −60, +60 mV, and −60 mV from a holding potential of 0 mV (insert). The zero current level is indicated by a dashed line. Currents measured in the absence of cyclic nucleotides were subtracted from data shown. (A) $CNGA1_{cys\text{-}free}$; bars: 1 nA, 20 ms. (B) M397C; bars: 1 nA, 20 ms. (C) T389C; bars: 50 pA, 20 ms. (D) I386C; bars: 50 pA, 20 ms.

(I_{cAMP}/I_{cGMP} = 0.07 ± 0.01; n = 7, red trace). This cyclic nucleotide specificity results from a change in the single-channel open probability and not a change in single-channel amplitude (Sunderman and Zagotta, 1999). Since these currents were measured in response to saturating concentrations of agonists, when binding sites were maximally occupied, the different current levels reflect differences in agonist efficacy for opening the channels. If we assume that the opening transition for a channel fully bound by agonist can be described by a simple closed-to-open equilibrium with equilibrium constant (L) then the behavior of the different agonists can be explained by L values specific for each agonist (L_{cGMP}, L_{cIMP}, and L_{cAMP}; Scheme I).

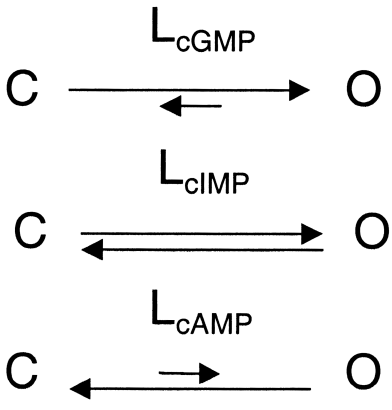

SCHEME I

The values of these equilibrium constants for $CNGA1_{cys\text{-}free}$ channels at 60 mV are shown in Table I. From the equilibrium constants, free energy differences between the closed and open states for $CNGA1_{cys\text{-}free}$ channels were calculated for each cyclic nucleotide using the relation $\Delta G_{L,cNMP} = -RT\ln(L_{cNMP})$. These free energies are slightly lower (0.8 kcal/mol) than reported previously for CNGA1 channels and suggest that removal of endogenous cysteines caused a small stabilization in the opening transition but did not affect the agonist specificity (Varnum et al., 1995; Varnum and Zagotta, 1996; Matulef et al., 1999; Sunderman and Zagotta, 1999; Flynn and Zagotta, 2001; Johnson and Zagotta, 2001; Matulef and Zagotta, 2002).

Cyclic nucleotide–activated currents in all cysteine mutant channels showed a similar order of agonist efficacy as $CNGA1_{cys\text{-}free}$; however, the magnitude of the efficacies were different. Fig. 3 shows examples of cyclic nucleotide–activated currents for three mutant channels. At some positions, cysteine replacement resulted in an increase in the fraction of current activated by cIMP and cAMP relative to cGMP, e.g., M397C. At other positions, cysteine replacement resulted in a decrease in the fraction of current activated by cIMP and cAMP, e.g., T389C. At still other positions the mutation had little or no effect, e.g., I386C. Assuming that the opening conformational change outside the CNBD,

TABLE I

Equilibrium Constants and Free Energy Differences for the Opening Transition of CNGA1$_{cys\text{-}free}$ Channels

CNGA1$_{cys\text{-}free}$	$L_{cNMP,+60\ mV}$	$\Delta G_{cNMP,+60\ mV}$
cGMP	72 ± 13[a]	−2.4 ± 0.12[a]
cIMP	4.3 ± 0.56	−0.83 ± 0.069
cAMP	0.092 ± 0.013	1.4 ± 0.084

Parameters were calculated as described in MATERIALS AND METHODS and are shown as mean ± SEM (n = 7).
[a]From Johnson and Zagotta (2001) (n = 12).

e.g., the conformational change in the pore, is similar for the different cyclic nucleotides, the mutations are expected to have a similar energetic effect on channel opening for all three agonists. Consistent with this interpretation, the variation in agonist efficacies observed among the different mutant channels could be accounted for by a constant energy change ($\Delta\Delta G_{L,mutation}$) in $\Delta G_{L,cGMP}$, $\Delta G_{L,cIMP}$, and $\Delta G_{L,cAMP}$. For example, the increase in the fraction of current activated by cIMP and cAMP relative to cGMP in M397C channels can be accounted for by a decrease in the free energy of the opening transition by the same amount for all three cyclic nucleotides.

For each of the mutant channels, we determined the energetic effect on opening. For these determinations, we assumed a fixed nucleotide specificity ($\Delta G_{L,cIMP} - \Delta G_{L,cGMP} = 1.7$ kcal/mol and $\Delta G_{L,cAMP} - \Delta G_{L,cGMP} = 4.0$ kcal/mol; Table I). These energies accurately account for differences in the amplitudes of cyclic nucleotide–activated currents of numerous mutant CNG channels where the mutations occurred at residues outside of the binding domain (Gordon and Zagotta, 1995a; Johnson and Zagotta, 2001). The maximum current (I_{max}) and the free energy difference of the opening transition in the presence of cGMP ($\Delta G_{L,cGMP}$) were determined by simultaneously fitting the amplitudes of cyclic nucleotide–activated currents with the above model (Scheme I) using the method of least squares. For G395C channels, cysteine replacement resulted in a channel with such an unfavorable opening transition that $\Delta G_{L,cGMP}$ was calculated as described in MATERIALS AND METHODS. The $\Delta G_{L,cGMP}$ values for each mutation were used to calculate the change in free energy of the closed-to-open transition caused by cysteine replacement using the relationship $\Delta\Delta G_{L,mutation} = \Delta G_{L,mutation} - \Delta G_{L,cys\text{-}free}$ (Fig. 4). As suggested by the apparent increase in the fractional activation by cIMP and cAMP in M397C channels, a cysteine at this site decreased the free energy difference of channel opening (−2.4 ± 0.06 kcal/mol, n = 5) shifting the equilibrium in favor of the open state. In contrast, a cysteine at T389C increased the free energy difference of channel opening (1.9 ± 0.062 kcal/mol, n = 4). For two positions, I390C and V391C (gray), a cysteine produced no significant difference in the channel opening transition compared with CNGA1$_{cys\text{-}free}$ as determined by Student's t test ($P > 0.2$; for all other sites $P < 0.005$). From these data it is clear that mutations in the S6 perturbed the gating equilibrium in both directions, in favor of the open state (green) and in favor of the closed state (red) (Fig. 4).

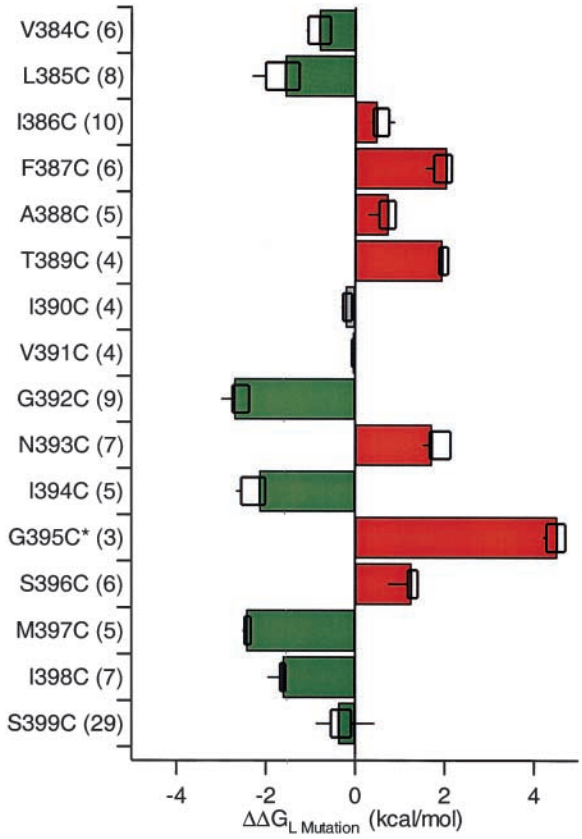

FIGURE 4. Changes in the free energy of channel opening ($\Delta\Delta G_{L,mutation}$) with cysteine replacement in the S6. Box plots of $\Delta\Delta G_{L,mutation}$ values for each mutant channel. For each box, the centerline is the median value, the edges of the boxes are the 25th and 75th percentiles, and the lines extending from the boxes are the 5th and 95th percentiles. Box plots were superimposed onto bar graphs extending for 0 to median $\Delta\Delta G_{L,mutation}$ for each mutant channel. Decreases (green) or increases (red) in $\Delta\Delta G_{L,mutation}$ relative to CNGA1$_{cys\text{-}free}$ are shown. Number of patches included in statistics is indicated in parentheses to the right of the mutant name.

Modification of S6 Cysteines Alters Gating and Permeation

We applied MTSEA to CNGA1$_{cys\text{-}free}$ channels and each of the 16 mutant channels and measured its effects on currents activated by the three cyclic nucleotides. MTSEA was applied in the presence of saturating cGMP to the intracellular side of patches. Currents were measured before exposure to MTSEA and after modification reached steady-state, when no further change in current

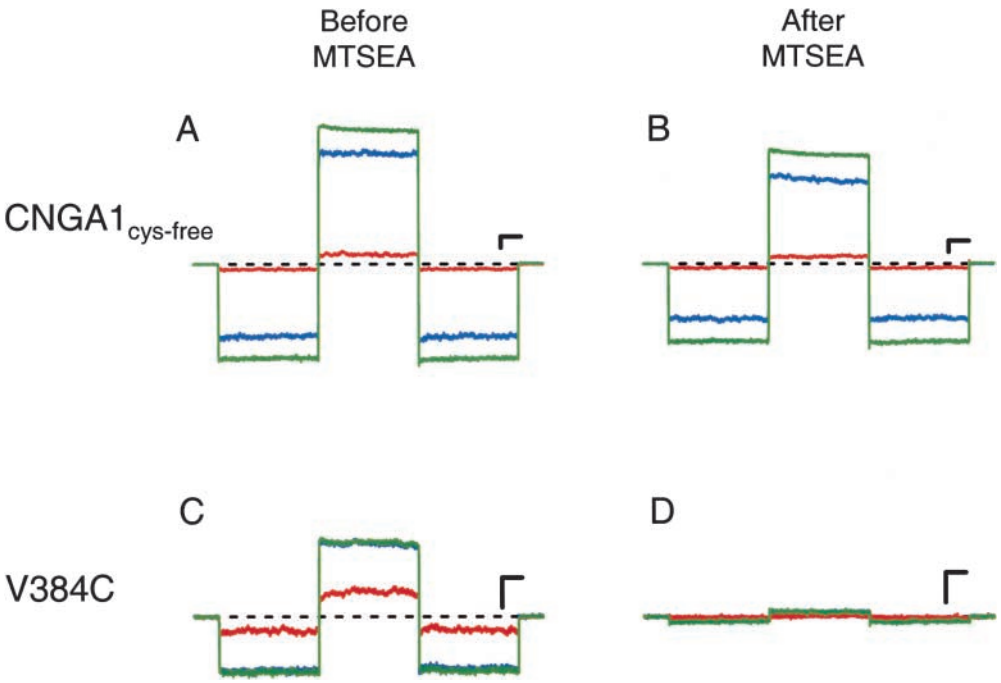

FIGURE 5. Cyclic nucleotide–activated currents in $CNGA1_{cys\text{-}free}$ and V384C channels before and after modification by MTSEA. Representative currents traces are shown from $CNGA1_{cys\text{-}free}$ and V384C channels activated by saturating concentrations of cGMP (green; 2.5 mM), cIMP (blue; 16 mM), and cAMP (red; 16 mM) in response to a three step voltage protocol (see insert Fig. 3). (A and B) Representative currents are shown for $CNGA1_{cys\text{-}free}$ channels before and after 2 mM MTSEA was applied to the intracellular side while channels were held in the open state by 2.5 mM cGMP. The cumulative exposure time was 10 min. Bars: 100 pA, 20 ms (C and D) Representative currents are shown for V384C channels before and after 200 μM MTSEA was applied in the open state for a cumulative exposure time of 13 min. Bars: 100 pA, 20 ms.

amplitude was observed. For $CNGA1_{cys\text{-}free}$ channels a cumulative exposure of 10 min to 2 mM MTSEA had negligible effects on the amplitude of current activated by each of the three cyclic nucleotides (Fig. 5, A and B). Small decreases in current were attributed to nonspecific effects and channel rundown that accompanied long recording times, i.e., patches held over 1 h.

In contrast to $CNGA1_{cys\text{-}free}$ channels, MTSEA produced a significant change in the current amplitude for many of the cysteine mutant channels. For example, a significant decrease in current occurred when 200 μM MTSEA was applied to V384C channels for 13 min (Fig. 5, C and D). To further characterize the functional effects of MTSEA, the time course of modifica-

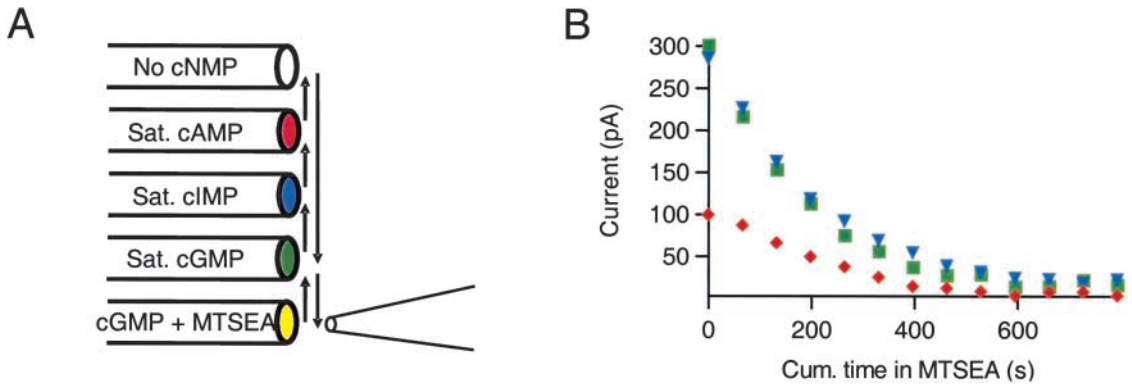

FIGURE 6. Time course of cysteine modification in V384C channels. (A) Schematic diagram showing the solution-switching protocol for applying MTSEA in the open state of mutant channels. The intracellular side of a patch was exposed briefly to a solution of 2.5 mM cGMP containing MTSEA for ~5–10 s. After each exposure, patches were washed in cGMP alone for 10 s. Currents were recorded in the presence of 2.5 mM cGMP, 16 mM cIMP, 16 mM cAMP, and 0 cNMP. Patches were exposed repeatedly to MTSEA for brief periods until no further change in current was observed. (B) Time course of modification by 200 μM MTSEA of V384C channels. Currents measured in cGMP (green square), cIMP (blue triangle), and cAMP (red diamond) at 60 mV were leak subtracted then plotted as a function of cumulative exposure time to MTSEA. Data are from the same patch as those shown in Fig. 5, C and D.

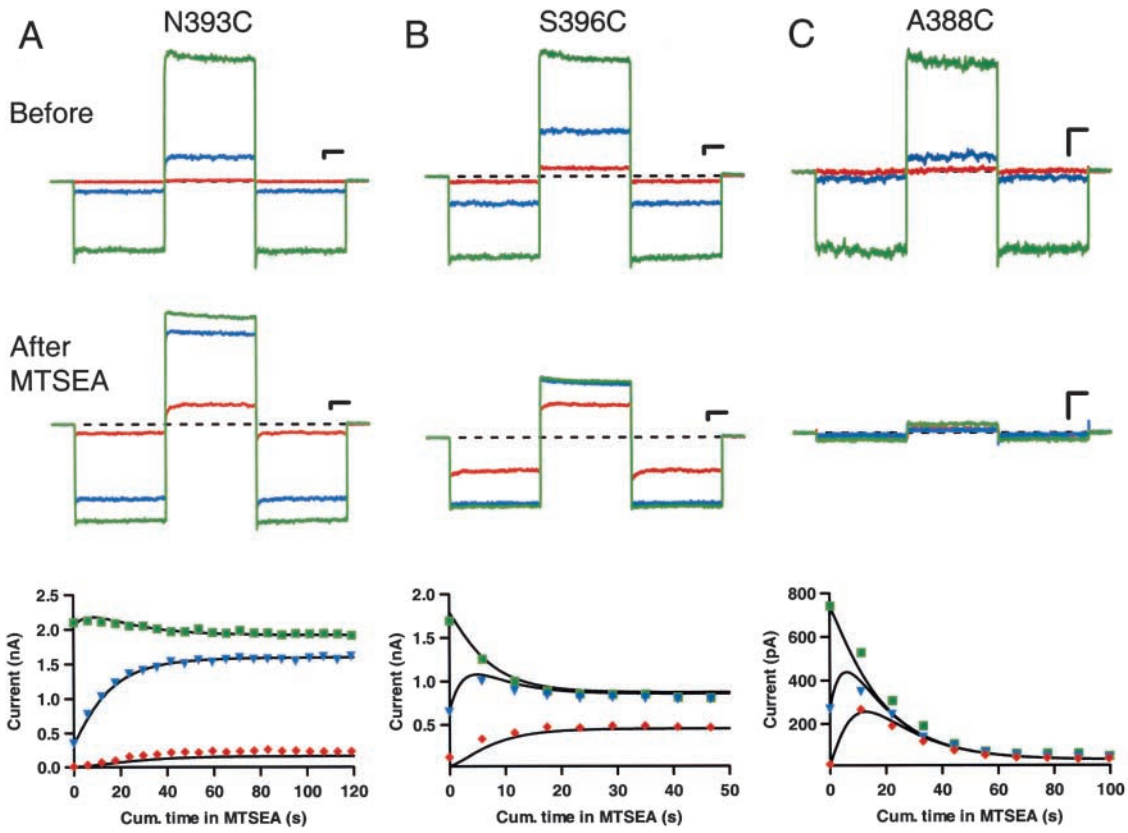

FIGURE 7. Complex kinetics of cysteine modification. (A) Representative currents are shown for N393C channels before (top) and after 2 min cumulative exposure to 20 μM MTSEA (middle). Plot of leak subtracted currents measured for each cyclic nucleotide recorded at 60 mV as a function of cumulative exposure time in MTSEA (bottom) is shown. Smooth lines through the data are from the model described in Fig. 8. Bars: 100 pA and 20 ms. (B) Currents recorded from S396C channels before and after 1 min cumulative exposure to 2 μM MTSEA. (C) Currents recorded from A388C channels before and after 100 s cumulative exposure to 20 μM MTSEA.

tion was determined for each mutant channel. The experimental design involved briefly exposing the intracellular side of mutant channels in excised inside-out patches to MTSEA in a saturating cGMP solution, washing the patches in saturating cGMP, and recording the current amplitudes activated by all three cyclic nucleotide at 60 mV (Fig. 6). This cycle was repeated until no further change occurred. By plotting current amplitudes for each of the cyclic nucleotides as a function of cumulative exposure time to MTSEA, the time course of cysteine modification was determined (Fig. 6 B).

While the effects of MTSEA on V384C channels simply decreased currents (Fig. 6 B), modification of other S6 mutant channels produced more complex effects. MTSEA caused cIMP- and cAMP-activated currents through N393C channels to increase while cGMP-activated currents appeared unchanged (Fig. 7 A). Oddly, cGMP-activated currents through S396C channels became smaller with modification while cIMP- and cAMP-activated currents became larger (Fig. 7 B). In A388C channels, MTSEA completely inhibited currents activated by all three cyclic nucleotides; however, the time course of modification was biphasic for cIMP- and cAMP-activated currents that initially increased and then decreased in amplitude (Fig. 7 C, bottom). In contrast, modification of A388C channels caused cGMP-activated currents to decay exponentially. The increase in cIMP- and cAMP-activated currents with modification strongly implied that the equilibrium constant for the opening transition was increased by modification, whereas the concomitant decrease in cGMP-activated currents suggested that modification was also interfering with permeation.

The complex effects of MTSEA modification could be reproduced by a model where modification alters both gating and permeation (Fig. 8). The model predicts the time course of the changes in current for all three cyclic nucleotides caused by modifying each of four possible cysteines within the channel. Inherent in the model are six assumptions. (1) For each modified form of the channel the gating behavior in saturating cyclic nucleotides can be described by a two state scheme as discussed above (Scheme I). (2) Modification follows a single exponential time course with a

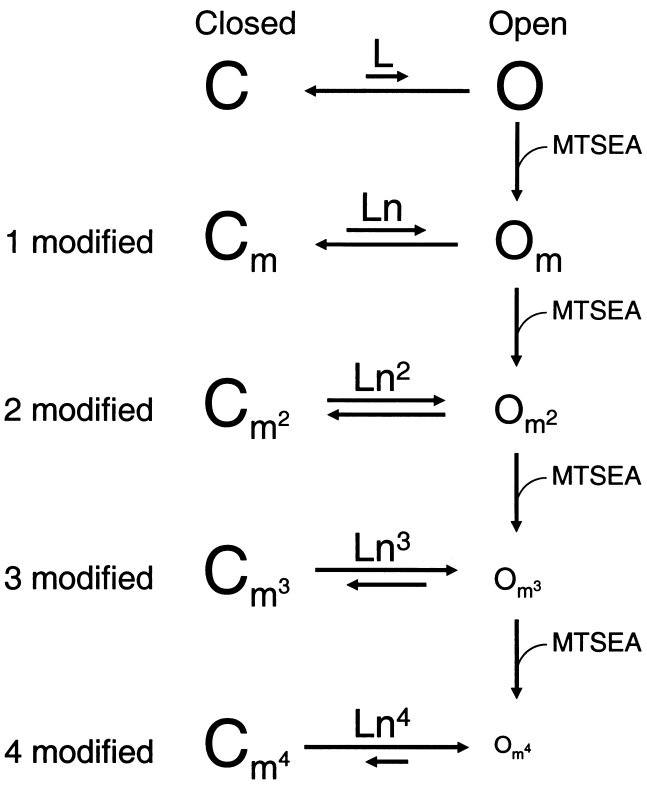

FIGURE 8. Kinetic model describing permeation and gating effects of cysteine modification. A model that predicts the time course of the changes in current for all three cyclic nucleotides caused by modifying each of four possible cysteines within the channel. The model is used to quantify the fractional change (n) in the equilibrium constant (L) between the closed (C) and open (O) states and the concomitant decrease in conductance through the open channel with each modification (m).

time constant, τ. (3) Each cysteine is modified independently resulting in a binomial distribution of the modified forms of the channel. (4) Effects of modification are equivalent for each of the four cysteines in any given channel. (5) Each modification of the channel contributes an equal and identical energy change to the closed-to-open transition as expected for a concerted conformational change involving all four subunits. This change in gating is described by a fractional change in the equilibrium constant for channel opening (n). (6) Each modification of the channel changes the conductance by a constant fraction (g). Although there is no theoretical basis for this last assumption, it has been shown previously that MTS reagents linearly decreased the single-channel conductance in inward rectifier (IRK) channels (Lu et al., 1999).

In an effort to justify the assumption that modification causes a linear reduction in conductance, we examined the extent of 2-trimethylammonioethylmethane thiosulfonate hydrochloride (MTSET) modification of S399C subunits in channels with two (heterodimers) or four (homodimers) cysteines. In homodimers all four subunits contained a S399C mutation, whereas in heterodimers two subunits contained S399C mutations and two subunits were $CNGA1_{cys\text{-}free}$. Both channel types were modified in the open state by applying to the cytoplasmic surface 200 μM MTSET in combination with 2.5 mM cGMP. MTSET caused macroscopic current levels in both heterodimers and homodimers to decrease to a new steady-state level (Fig. 9 A). Modification produced a twofold greater reduction in current in homodimers relative to heterodimers (Fig. 9, A and B). These results agree with our assumption that modification of each cysteine in S399C channels decreases the conductance by a constant fraction. While it may be true that the assumption of linear reduction in conductance does not hold for every S6 position, the success of the model in fitting the data at most positions suggests that this assumption is valid to a first approximation.

For each of the 16 mutant channels, fits of the model to the time course data were used to quantify the observed changes. The model contains three free parameters: (a) the bimolecular rate constant for modification of a single cysteine [rate constant = 1/(τ/[MTSEA])], (b) the fractional change in conductance for each modification (g), and (c) the fractional change in the equilibrium constant for the closed-to-open transition for each modification (n). Smooth lines in Fig. 7 are fits of the model to the modification time courses of N393C, S396C, and A388C for all three cyclic nucleotides. For most mutant channels, the model successfully described the complex time course of the currents that results from cysteine modification. The exceptions were G395C and S399C channels which exhibited responses to modification that were not well described by this model. These modification effects will be discussed in more detail at the end of the RESULTS section.

Open-state Accessibility of S6 Residues

One way to determine which residues line the pore is to quantify the accessibility of residues to cysteine modification. We investigated the open-state accessibility of the S6 residues by quantifying the second-order rate constants of MTSEA modification for each mutant channel. In the open state, S6 residues with side chains directed toward the center of the pore were predicted to modify more rapidly with MTSEA than residues with side chains directed away from the pore. From the time courses of modification of each mutant channel, time constants were determined from fits of our model to the time course data as described above. The inverse of τ was divided by the MTSEA concentration used to modify each mutant channel in order to obtain a second-order rate constant of modification for that site. Rate constants corresponding to each S6 site are plotted as box plots in

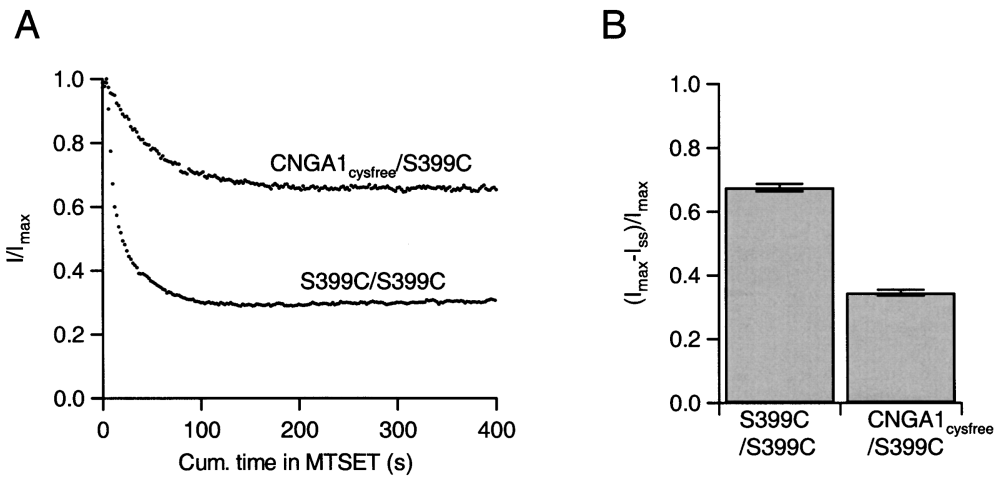

FIGURE 9. Effect of MTSET modification is reduced twofold in heterodimeric $CNGA1_{cys\text{-}free}$/S399C channels. (A) Time course of MTSET modification of S399C/S399C homodimers and $CNGA1_{cys\text{-}free}$/S399C heterodimers. A 2.5 mM cGMP solution containing 200 μM MTSET was applied to the intracellular side of each patch. Current amplitudes were normalized to the maximum cGMP-activated current for each patch. (B) Fraction of current modified by MTSET for homodimers and heterodimers. Bars show mean ± SEM ($n = 3$).

Fig. 10 A. We found that most of the residues between 384 and 399 were accessible to MTSEA modification in the open state. Notable exceptions were L385C and I386C (white boxes) where the effects of MTSEA were not significantly different from that of $CNGA1_{cys\text{-}free}$ channels ($P > 0.05$; Student's t test). Superimposed on these data is the sine function from Fig. 2 B that describes the angle of rotation of the β carbons in KcsA and MthK relative to the pore axis. The data in Fig. 10 A are consistent with the sequence alignment shown in Fig. 1 and show that pore-lining residues were modified more rapidly by MTSEA then other S6 residues.

Shown in Fig. 10 B are two homology models of the CNGA1 S6 region based on the crystallographic coordinates of KcsA and MthK, respectively (Doyle et al., 1998; Jiang et al., 2002b), and the sequence alignment in Fig. 1. The KcsA model represents the putative closed state of the channel and the MthK model represents the open state. The S6 positions with median rate constants greater than 10^4 $M^{-1}s^{-1}$ are shown in red, between 10^3/

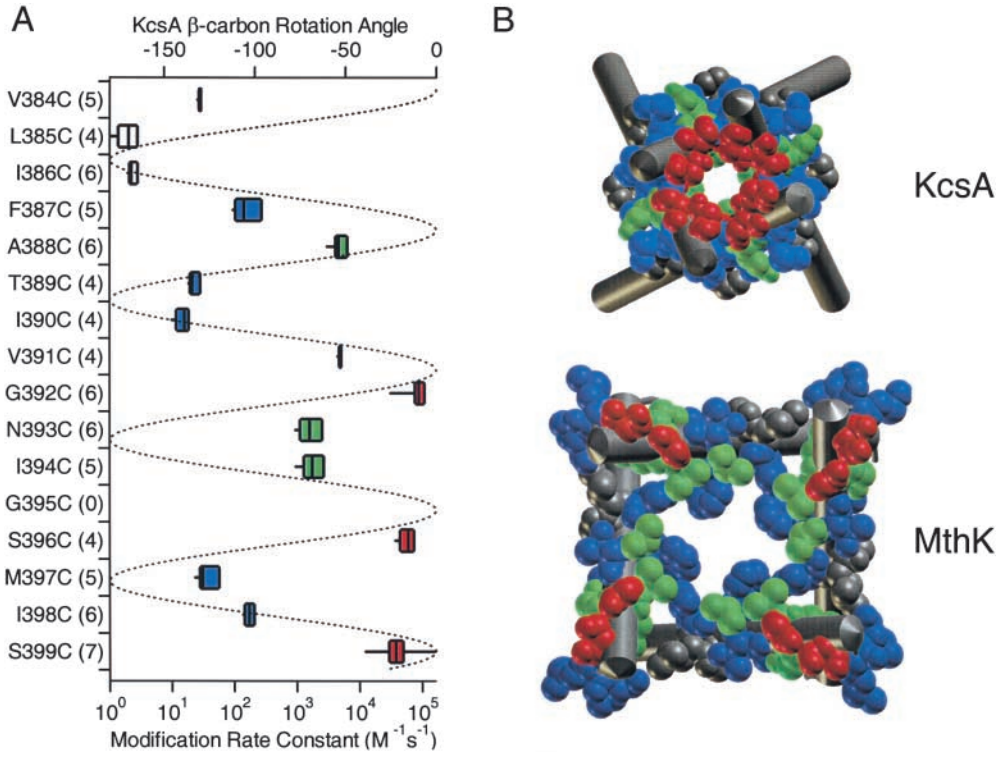

FIGURE 10. Rate constants of open-state cysteine modification for each S6 position. (A) Box plots of the bimolecular rate constants of MTSEA modification for each mutant channel. Dashed line is the sine function fit to the KcsA and MthK rotation angle data from Fig. 2. Colors correspond to median rate constants $>10^4$ $M^{-1}s^{-1}$ (red), between 10^3 $M^{-1}s^{-1}$ and 10^4/M/s (green), and between 10^1 $M^{-1}s^{-1}$ and 10^3 $M^{-1}s^{-1}$ (blue). Rate constants for L385C and I386C channels (white) were not statistically different from $CNGA1_{cys\text{-}free}$ (Student's t test, $P > 0.6$). (B) Homology models showing a bottom view of four S6 helices based on KcsA (top) and MthK (bottom), representing the closed and open conformations respectively. Sites corresponding to CNGA1 positions 384–399 are shown as space filled. Colors correspond to data in A.

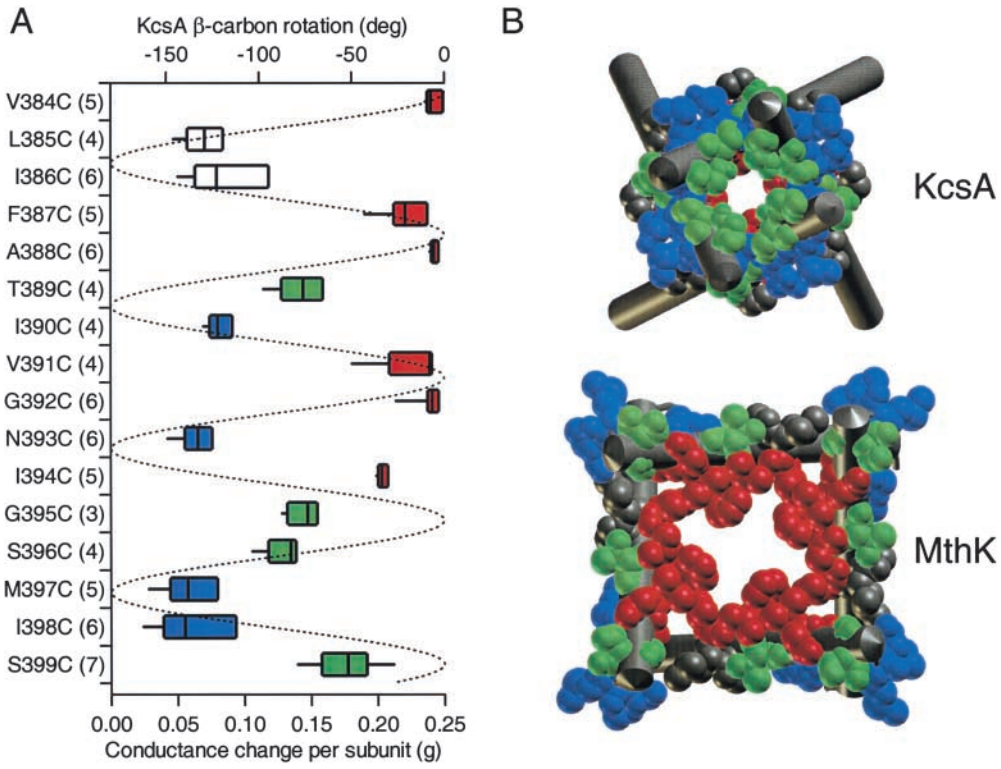

FIGURE 11. Changes in conductance due to MTSEA modification of S6 cysteines. (A) Box plots of the fractional conductance change per subunit (g) at 60 mV for each mutant channel determined from the model in Fig. 8. Dashed line is the sine function fit to the KcsA and MthK rotation angle data from Fig. 2. Colors correspond to median g values greater than 0.20 (red), between 0.10 and 0.20 (green), and <0.10 (blue). Because the rate constants of modification of L385C and I386C channels were not statistically different from $CNGA1_{cys\text{-}free}$, box plots for these sites are shown in white. (B) Homology models showing sites color coded to correspond with data in A.

M/s and 10^4 $M^{-1}s^{-1}$ are shown in green, and between 10^1 $M^{-1}s^{-1}$ and 10^3 $M^{-1}s^{-1}$ are shown in blue. Rate constants for L385C and I386C channels (white) were not statistically different from $CNGA1_{cys\text{-}free}$ (Student's *t* test, $P > 0.6$) (Fig. 10). In general, the residues lining the pore are the most rapidly modified for both homology models, but there are exceptions. One obvious exception occurs at F387, which when replaced by a cysteine, was modified at a rate slower than expected for that position. This result may be the consequence of the site residing relatively deep in the pore where accessibility may be electrostatically and sterically hindered. This may also be true for V384C, which modified much slower than expected for a pore-lining residue. V384C is located deep within the pore just one amino acid after a conserved glycine which, in MthK, forms a kink in the inner helix (Jiang et al., 2002b). Interestingly, the rate constants for modification of N393C and I394C channels were higher than predicted by the sine function and the homology models. These results suggest that there may be a "hole" open to the cytoplasm on the back side of the S6 helix near N393 and I394 (Fig. 10). On the other hand, MTSEA is membrane permeant and modification within the membrane is possible. However, we also found that N393C channels were modified by MTSET (2-trimethylammonioethylmethane thiosulfonate hydrochloride), a membrane-impermeant cysteine modifier, which is further evidence for an aqueous hole (unpublished data). In general, the rate constants were consistent with an α helical pattern in the accessibility of S6 sites; however, other factors in addition to lining the pore can influence these rates.

MTSEA Modifies Permeation

Another way to determine which residues line the pore is to quantify the effects of modification on permeation. The largest conductance changes are expected for pore-lining residues from an electrostatic interaction between the positive charge on the modified cysteine and the permeant cations. One of the parameters of our model described the relative change in conductance caused by cysteine modification. In the model, we assumed that cysteine modification caused an identical change in all four subunits and that the effects of modification on conductance were additive. The fractional change in conductance per subunit due to modification (g) for each mutant channel is plotted relative to the amino acid number in Fig. 11 A. The sites with the largest MTSEA effect on the fractional conductance were those predicted by the sequence alignment and the homology models to project side chains toward the pore axis. When the g values from the kinetic model were mapped onto the homology models, the sites lining the pore were associated with the largest conductance changes (Fig. 11 B, red). These results are consistent with work published earlier describing the inhibitory effects of MTSET on some of these same mutant channels (Flynn and Zagotta, 2001). These effects on conductance were more indicative of pore-lining

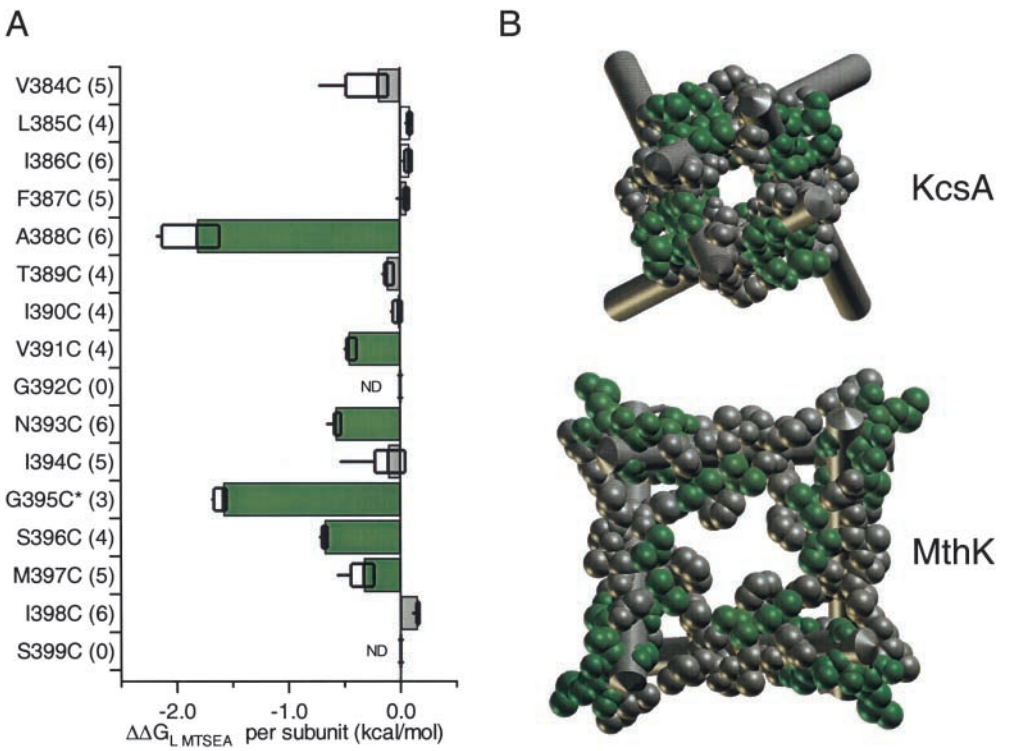

FIGURE 12. Changes in the free energy of channel opening ($\Delta\Delta G_{L,MTSEA}$) with MTSEA modification of S6 cysteines. (A) Box plots and bar graphs of $\Delta\Delta G_{L,MTSEA}$ values per subunit determined for each mutant channel from the model in Fig. 8. Sites with a statistically significant decrease in the free energy change for the opening transition are shown in green. ND, not determined. (B) Homology models showing sites color coded to correspond with data in A.

residues than the accessibility measurements. For example, MTSEA modification of the pore-lining residues F387C and V384C, which had slow rates, dramatically affected the conductance. Therefore, we conclude, from the data in Figs. 10 and 11, that the region between 384 and 399 of CNGA1 channels is an unbroken α helix that lines the pore similar to KcsA and MthK. Perhaps more interestingly, pore-facing residues at the cytoplasmic end of the S6 (positions 395 and 399) had a somewhat smaller effect on conductance than expected for residues lining the pore. The 399 position in the KcsA homology model is within 4 Å from the central pore axis compared with 15 Å in the MthK homology model. The effect of modification on conductance at this position, therefore, is more consistent with a structural similarity between the open state of CNGA1 and MthK.

Cysteine Modification in S6 Alters Gating Equilibrium

The sensitivity of the closed-to-open equilibrium to cysteine modification provides useful information about the energetic and structural changes that occur during gating. Alterations in gating result from a differential effect of modification on the stability of the closed and open states. They therefore reflect the relative movement of the modification site during gating. One parameter of our model described the fractional change in the equilibrium constant for the opening transition (n) due to cysteine modification of each subunit. From these n values, we calculated the energetic effects of modification on the closed-to-open transition from the relationship $\Delta\Delta G_{L,MTSEA} = -RT\ln(n)$ (Fig. 12). At eight S6 sites, MTSEA had no appreciable affect on the equilibrium of channel opening. At six other sites, however, MTSEA modification decreased the free energy of channel opening, resulting in a shift in the equilibrium of channel opening in favor of the open state (Fig. 12, green bars; $P > 0.0005$). The largest effects were at A388C and G395C predicted by the sequence alignments (Fig. 1) and homology models to be pointing toward the center of the pore (Fig. 12 B). A possible interpretation of these results is that the four S6 helices are very close together in this region in the closed state and electrostatic interactions between positive charges on the modified cysteine residues may serve to push the helices apart. Not all the sites affected by the modification were facing the pore. Residues N393C, S396C, and M397C were located in a pocket on the back of the S6 helix pointing away from the pore (Fig. 12 B). One interpretation of these results arises if we consider the KcsA and MthK structures as models for the closed and open state conformations for CNGA1 channels (Jiang et al., 2002b). The added volumes of the modified cysteines may preferentially destabilize the tight helical packing of the closed state conformation seen in KcsA relative to the looser packing of the open state conformation seen in MthK. A similar mechanism has been proposed for Shaker K^+ channels (Yifrach and MacKinnon, 2002).

Replacing the glycine at position 395 with cysteine

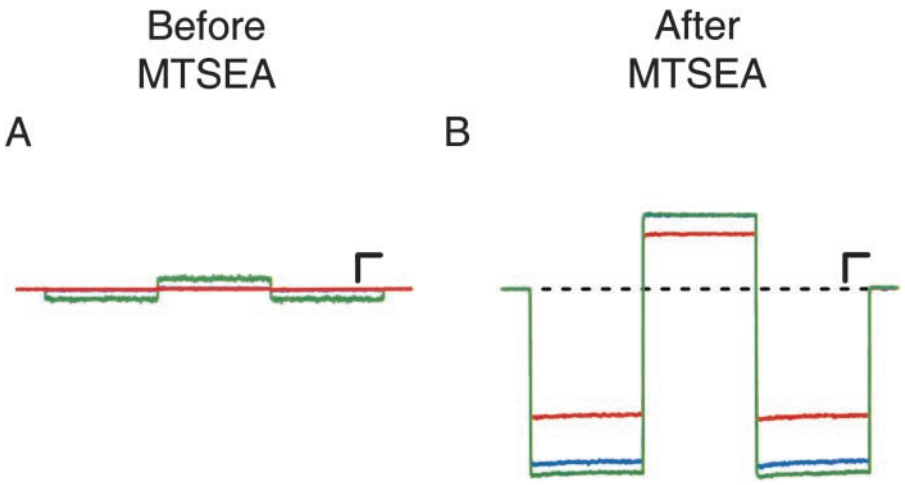

FIGURE 13. MTSEA modification of G395C channels causes potentiation of cyclic nucleotide–activated currents. Representative currents for G395C channels before (A) and after (B) 2 mM MTSEA in 2.5 mM cGMP was applied to the intracellular side for 2 min. Bars: 200 pA, 20 ms.

produced a channel with such a low open probability that the cGMP-activated currents were small and cIMP- and cAMP-activated currents were indiscernible from leak currents (Fig. 13 A). However, dramatic increases in the currents activated by all three cyclic nucleotides and a pronounced inward rectification were observed after MTSEA modification (Fig. 13 B). This behavior reflects a profoundly unfavorable opening transition before modification and a favorable opening transition after modification. The positive charge on the modified cysteine appears to interfere with the permeation of cations in the outward direction but not the inward direction. The model in Fig. 8 was not used and n was determined as discussed in MATERIALS AND METHODS.

Some Mutations/Modifications Produce Unliganded Openings

The model in Fig. 8 considered the opening of channels when fully bound by ligand. However, channels might be expected to open in the absence of ligand if a large decrease in the free energy of opening occurred. We observed such an increase in current measured in the absence of ligand during MTSEA modification of A388C channels, the mutant channel with the largest gating effect due to modification (Fig. 12 A). Modification of A388C channels produced a transient increase in the current measured in the absence of ligand (Fig. 14). This current could not be attributed to slow patch perfusion or slow unbinding of cyclic nucleotide (unpublished data). The probability that modified A388C channels are opened in the absence of ligand can be estimated from the ratio of the spontaneous current to the cGMP-activated current (I_{sp}/I_{cGMP}; Fig. 14 B). This ratio increased exponentially to a steady-state level of 0.44 ± 0.071 ($n = 6$). These results suggest that the cysteine modification of A388C produced such a large decrease in the free energy of opening that the channels were open in the absence of ligand.

A large decrease in the free energy of opening also occurred as a consequence of mutation. G392C channels had the largest equilibrium constant for channel opening of any mutant channel in this study (L_{cGMP} =

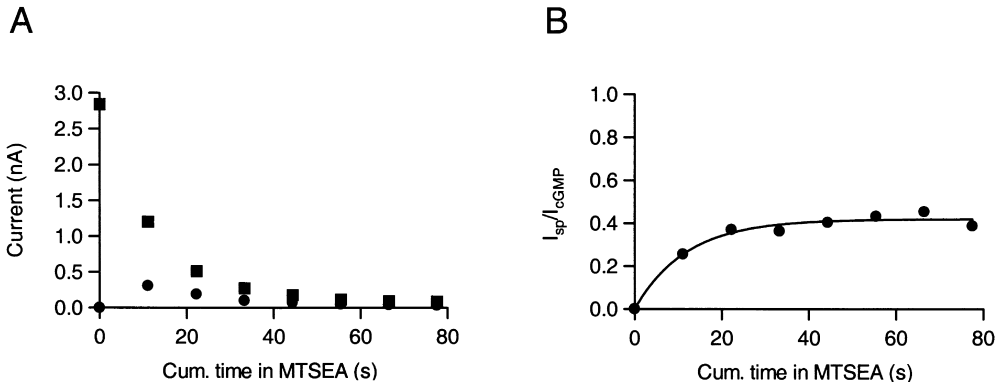

FIGURE 14. Unliganded openings observed with large increases in the opening equilibrium constant after MTSEA modification. (A) Time course of modification by 20 μM MTSEA of A388C channels. Currents were measured at 60 mV, leak subtracted, and plotted as a function of cumulative exposure time to MTSEA. Shown are current amplitudes measured in 2.5 mM cGMP (I_{cGMP}) (square) and current amplitudes measured in the absence of cyclic nucleotide (I_{sp}) (circles). (B) Ratio I_{sp}/I_{cGMP} is plotted as a function of cumulative exposure time to MTSEA. Smooth line is a single exponential fit to the data of the equation $I_{sp}/I_{cGMP} = 0.42 - 0.42e^{(-0.084t)}$, where t is time.

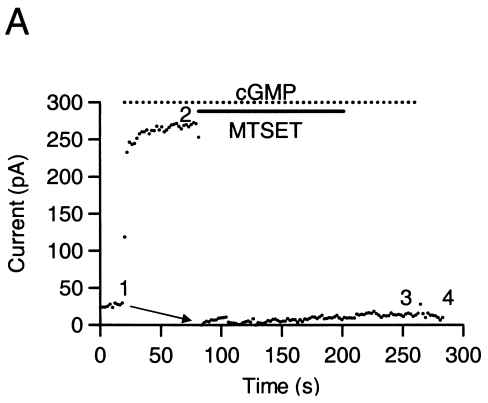

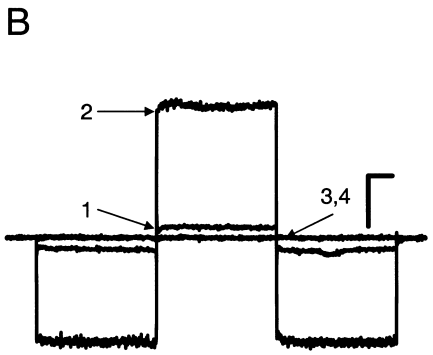

FIGURE 15. Cysteine modification shows a high probability of unliganded openings for G392C channels. (A) Current amplitudes measured at +60 mV in the absence and presence of cyclic nucleotide. The solid line indicates the time when 2 mM MTSET in 2.5 mM cGMP was applied to the patch. The dashed line indicates the time when 2.5 mM cGMP was applied. Arrow indicates the change in current through unliganded channels. (B) Selected current traces showing the effects of MTSET modification on currents. Shown are currents in the absence of cyclic nucleotide (arrows 1 and 4) and in cGMP (arrows 2 and 3). Numbers correspond to points in A. Bars: 100 pA, 20 ms.

6,685 ± 1,073; $n = 9$), ~2 orders of magnitude larger than the equilibrium constant for $CNGA1_{cys\text{-}free}$ channels ($L_{cGMP} = 72 \pm 13$; $n = 12$). We observed that when 2 mM MTSET was applied to G392C channels there was a rapid decline in all currents to a level below that measured in the absence of cyclic nucleotide (Fig. 15 A). A similar decrease in current was observed when G392C channels were modified with MTSEA (unpublished data). This decrease in current measured in the absence of ligand was not observed with any other S6 mutant channels before modification or $CNGA1_{cys\text{-}free}$ channels. These results suggest that some of the leak current in the absence of cyclic nucleotide is due to spontaneous opening of G392C channels and is blocked by cysteine modification. The probability that G392C channels are opened in the absence of ligand as determined by the ratio of the spontaneous current (Fig. 15 B, arrow 1) to the cGMP-activated current (Fig. 15 B, arrow 2), is 0.070 ± 0.021 ($n = 3$). This mutational perturbation was the largest observed in the S6 region (Fig. 4).

Anomalous Effects of Modification

The time course of G395C channel modification revealed an additional complexity. Continuous modification by 20 μM MTSEA caused a large increase in the cGMP-activated current at −60 mV that followed a roughly exponential time course to a new steady-state level (Fig. 16 A). At a higher concentration, 2 mM MTSEA, the increase in cGMP-activated current at −60 mV

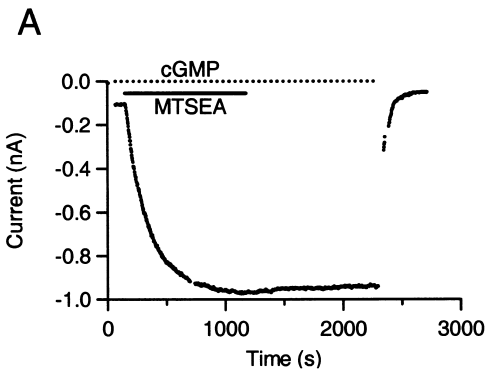

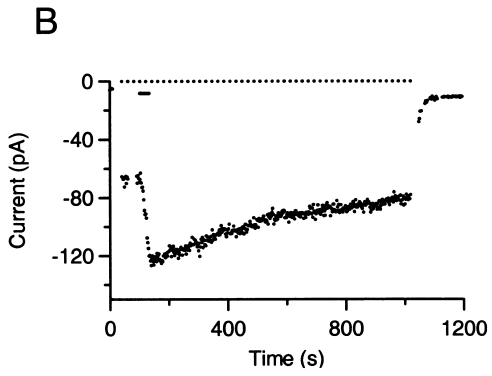

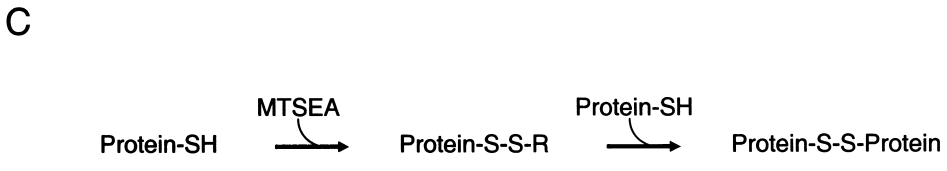

FIGURE 16. Partial MTSEA modification of G395C channels catalyzes thiol-disulfide exchange. (A) Current amplitudes measured at −60 mV while 2.5 mM cGMP was applied to the intracellular side of the patch (17 min, dashed line above the data). Currents were measured in 20 μM MTSEA in cGMP (solid line) until the effect reached steady-state. Amplitude of current measured in the absence of cyclic nucleotide is also shown. (B) Current amplitudes measured at −60 mV while 2.5 mM cGMP was applied (dashed line) to intracellular side of the patch. Currents were measured during a brief application (30 s, solid line) of 20 μM MTSEA in cGMP. (C) Reaction scheme depicting thiol-disulfide exchange.

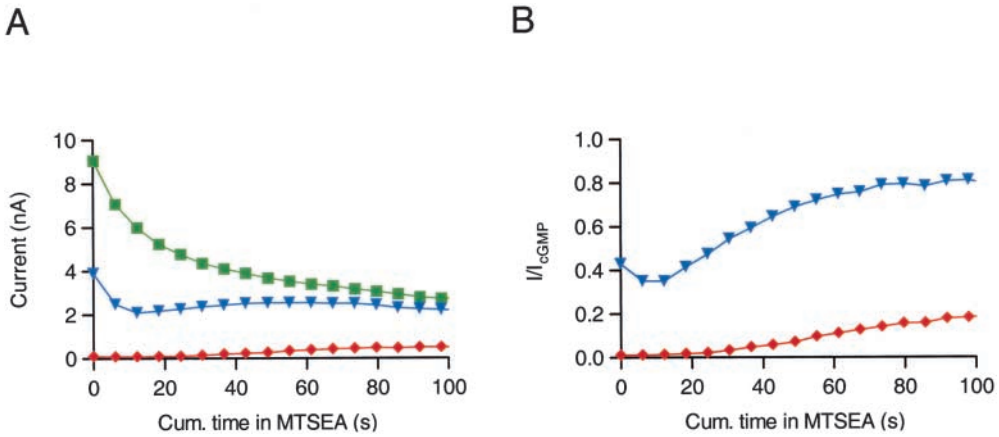

FIGURE 17. Cysteine modification of S399C channels shows an additional gating component. (A) Time course of modification by 2 μM MTSEA of S399C channels. Shown are current amplitudes measured in 2.5 mM cGMP (green square), 16 mM cIMP (blue triangles), and 16 mM cAMP (red diamonds). (B) Ratios I_{cIMP}/I_{cGMP} and I_{cAMP}/I_{cGMP} are plotted as a function of cumulative exposure time to MTSEA.

was 31-fold ± 7.7 (n = 3). However, we observed that after repeated brief applications of MTSEA little or no increase in current was observed (unpublished data). A possible interpretation to reconcile this paradoxical behavior was that during brief exposures to modifier there was sufficient time for the unmodified cysteines within the channel to undergo thiol-disulfide exchange with the MTSEA modified cysteines to form an intersubunit disulfide bond (Creighton, 1984). Thiol-disulfide exchange is a reaction between the mix disulfide of the modified cysteine and a free cysteine thiol-group to form a symmetrical disulfide bond (Fig. 16 C). In our case, thiol-disulfide exchange would result in an intersubunit disulfide bond suggesting that G395C residues from neighboring subunits are within 10 Å of each other. To test for thiol-disulfide exchange, we applied 20 μM MTSEA for a brief period (e.g., 20 s), allowing only partial modification. After partial modification, currents activated by cGMP spontaneously declined (Fig. 16 B). Our interpretation is that after partial modification some cysteines are left unmodified and are available to participate in thiol-disulfide exchange. However, in the continued presence of 20 μM MTSEA all possible sites become modified quickly and as a consequence there are no available unmodified cysteines to form an intersubunit disulfide bond. Consistent with this interpretation, S399C channels form a spontaneous intersubunit disulfide bond that eliminates the current (Flynn and Zagotta, 2001). Because of this complicated behavior, the effects of MTSEA modification on G395C channels were not analyzed using the model in Fig. 8.

Modification of S399C channels also revealed an additional complexity. During the time course of MTSEA modification, S399C channels exhibited an initial increase followed by a decrease in free energy of channel opening, in addition to an effect of permeation (Fig. 17 A). The complex gating effect is more clearly demonstrated by plotting the fractional activation, I_{cIMP}/I_{cGMP} and I_{cAMP}/I_{cGMP}, as a function of exposure time where the effects of permeation are removed (Fig. 17 B). The fractional activation by cIMP initially decreased and then increased, and the fractional activation by cAMP increased with a delay. If the effect of modification on gating were similar to that observed for other S6 mutants, we would expect the fractional activations to have a monotonic time course. An interpretation of these results is that partial modification causes an unfavorable change in the free energy of channel opening for S399C channels, but further modification causes a favorable change in the free energy of channel opening. Such a result could occur if modification of a single cysteine destabilizes channel opening but additional modifications cause electrostatic interactions to occur between modified cysteines destabilizing channel closing. A model incorporating these considerations was used to determine the bimolecular rate constant of modification (Fig. 10) and the fractional change in conductance per subunit for S399C channels (Fig. 11).

DISCUSSION

In this study, we investigated the architecture and rearrangement of the S6 region of a cysteine-free variant of CNGA1 channels. First, we studied how the CNGA1-gating mechanism was perturbed by S6 mutations. Next, we measured local accessibility of each residue in the open state and studied how gating and permeation were perturbed by cysteine-specific modification. Finally, we interpreted our results in terms of the known structures of KcsA and MthK.

Cysteine Replacement in S6 Affects Gating

Mutations alone provide little direct information about protein structure. However, the sensitivity of the closed-to-open equilibrium to mutations does provide information about the structural elements involved in gating. We observed both favorable and unfavorable energetic effects on the closed-to-open equilibrium as a result of cysteine replacement between positions 384 and 399

in the S6 region of CNGA1 channels. The gating process is sensitive to mutational perturbations in most of the S6 helix, suggesting that the S6 is involved in gating. However, there was no pattern to these effects that could be correlated to any structural elements. It is difficult to make direct comparisons of the energetic effects caused by mutations between different positions when the perturbations are different for each positions, i.e., each substitution involves a different starting residue. In this study, a direct comparison is made possible by comparing the energetic effects of modification between positions where all the perturbations were the same, i.e., cysteine to cysteine + modifier.

Gating effects of S6 mutations are not unique to CNG channels. In both the six transmembrane and two transmembrane families of P-loop–containing channels, mutations in the cytoplasmic half of the inner helix have been reported to alter gating (Shyng et al., 1997; Lu et al., 1999; Enkvetchakul et al., 2000; Lippiat et al., 2000; Li-Smerin et al., 2000; Loussouarn et al., 2000; Espinosa et al., 2001; Panchenko et al., 2001; Sadja et al., 2001; Hackos et al., 2002; Jin et al., 2002; Lu et al., 2002; Yifrach and MacKinnon, 2002). Mutations in the inner helix have been shown to have both favorable and unfavorable energetic effects on the closed-to-open equilibrium. In the most extreme cases, the energetic effects were so favorable that the channels were constitutively active (Minor et al., 1999; Yi et al., 2001a; Yi et al., 2001b; Sadja et al., 2001; Zeidner et al., 2001; Hackos et al., 2002). We show here that G392C, and A388C after modification, also make the channels open in the absence of ligand. These results suggest that the inner helix is important for channel gating of many P-loop–containing channels.

Some of the cysteine mutations in the S6 produced novel gating effects. Currents through S399C channels spontaneously declined immediately after patch excision. We demonstrated previously that the decline in S399C current is due to the formation of a disulfide bond between the S399C residues from different subunits (Flynn and Zagotta, 2001). An intersubunit disulfide bond also formed in V391C channels, but required the presence of the mild oxidizing agent copper: phenanthroline (Flynn and Zagotta, 2001). Currents through G395C channels decline after a brief exposure to MTSEA. This unexpected result suggests a possible disulfide bond between G395C residues that is catalyzed by thiol-disulfide exchange (Creighton, 1984). All of these results are consistent with the prediction that V391C, G395C, and S399C are pointing toward the center of the pore. The distance between each of these sites on neighboring or diagonal subunits is <10 Å in the KcsA homology model, which is within a suitable range for disulfide bond formation (Creighton, 1984, 1993; Falke et al., 1988; Careaga and Falke, 1992). Another novel gating effect is observed in A388C channels. Currents through A388C channels spontaneously decline to a new steady-state level when the patch was exposed to a saturating cGMP solution (unpublished data). This decline in current was partially recoverable when the channels were closed by exposure to a cyclic nucleotide-free solution. Thus, A388C channels desensitized.

Changes in Gating and Permeation Occur as S6 Cysteines are Modified

Many of the cysteine mutant CNG channels exhibited a complex response to modification by positively charged MTSEA when applied in the open state. We observed a decrease in cGMP-activated currents and a concomitant increase in cIMP- and cAMP-activated currents in several mutant channels. Because of these disparate effects on CNG currents, we designed a kinetic model that describes the effects of modification in terms of alterations in both gating and permeation. The model predicts changes in current for all three cyclic nucleotides caused by modifying each of four possible cysteines within the channel. Three key assumptions in the model were (a) each modification produced an equal and identical change in the free energy difference between the closed and open states, (b) each modification produced an equal and identical change in the conductance, and (c) each modification occurs independently. The first of these three assumptions is reasonable and is the prediction of a concerted opening conformational change. A number of mutations have been observed to have energetic effects that are nearly additive when different numbers of subunits are mutated (Liu et al., 1996, 1998; Varnum and Zagotta, 1996). However, it has also been proposed that CNG channels gate by a dimer-of-dimer mechanism where the energy effects are nonadditive (Liu et al., 1998). The first assumption is also violated if disulfide bonds occur or if there are interactions between modifiers, such as electrostatic interactions between positive charges. The second of these three assumptions is not well supported theoretically; however, it has been shown previously that modification by 1, 2, 3, or 4 MTS reagents produced an approximately linear decreased in the single-channel conductance (Lu et al., 1999; Loussouarn et al., 2001). It is also supported by the observation that the current decline due to MTSET modification of S399C is twofold less in heterodimeric channels in which the number of modifiable cysteines is reduced by two relative to homodimeric channels. For the third assumption, one possible violation occurs when modification is state dependent and produces a significant change in the open probability of the channel. In this study, all modification was performed by applying MTSEA in combination with a 2.5 mM concen-

tration of cGMP. The open probability of most of the mutant channels in 2.5 mM cGMP was near one, with the noted exception of G395C channels. In all cases where modification changed the open probability, the change increased an already high open probability for these channels. In addition, we have shown previously that residues deep in the pore (e.g., V391C) do not exhibit state-dependent modification by MTSEA (Flynn and Zagotta, 2001) and therefore state-dependent modification is not a significant issue. A second possible violation of the third assumption is that the rate of modification is affected by electrostatic or steric interactions from a previous modification. This seems likely for G395C and S399C channels where the model did not produce an adequate fit. However, the success of the model in fitting the data at most positions suggests that these assumptions are reasonable. These assumptions are required for the systematic analysis presented here, and we believe the qualitative conclusions reached in this study are not strongly dependent on the specifics of the model.

We used our model to analyze modification of cysteine residues introduced at positions 384–399 in the S6 of CNGA1 channels. By analyzing the effects of modification, we can directly compare the results from multiple positions with identical perturbations at each position. For each site, we determined three different properties of the modification: (a) the bimolecular rate of modification in the open state, (b) the change in conductance with modification, and (c) the change in the closed-to-open equilibrium with modification. In the open state, we observed modification rates that ranged over five orders of magnitude. The effects of modification on permeation ranged from little to complete, but were always negative thus resulting in a decrease in conductance. The effects of modification on the closed-to-open transition were variable but were always positive, thus increasing the cAMP-activated currents. The success of the model in fitting the data from a great majority of positions in the S6 suggests that the model provides a good description of the gating and permeation effects of modification.

Structural Homology with KcsA and MthK

CNGA1 channels share sequence similarity with KcsA and MthK channels. We have further confirmed a structural homology between these channels and CNGA1 channels by showing that CNGA1 residues predicted by these structures to point toward the center of the pore were those sites modified with the fastest rate constants (Fig. 10). We also found that changes in the fractional conductance per subunit caused by attaching a positively charged group to cysteine residues in the S6 region were largest for those sites predicted to point toward the center of the pore, as though the positively-charged cysteine interacted with the permeant ion (Fig. 11). Perhaps more interestingly, pore-facing residues at the cytoplasmic end of the S6 (positions 395 and 399) had a somewhat smaller effect on conductance than other residues lining the pore. This result is perhaps more consistent with a structural similarity between CNGA1 and MthK where the cytoplasmic end of the inner helix veers away from the central axis of the pore.

Nature of the Physical Changes in the S6 of CNGA1

The MthK structure was solved in the presence of a calcium ligand that shifts the opening transition of these channels to favor the open state (Jiang et al., 2002a,b). Superimposition of KcsA and MthK suggests a structural model for the closed-to-open transition in the inner helices; with KcsA being closed and MthK being open. The physical model suggests that in the closed state the inner helices are close together, forming a helical bundle on the cytoplasmic side of the channel (Doyle et al., 1998). In the open state, the inner helices are separated by a bend at a conserved glycine disrupting the helical bundle and widening the entrance to the pore (Jiang et al., 2002b). This glycine hinge is just one residue upstream of the region we investigated and may mark a site within CNG channels for a break or bend in the S6 helix.

A model where the inner helices separate during channel opening is consistent with our results. MTSEA modification of many S6 sites resulted in a decrease in free energy for channel opening (Fig. 12). This decrease might be caused if MTSEA disrupted the helical packing of the closed channel, making it easier for the channels to open. We have shown previously that S399C forms an intersubunit disulfide bond when channels are closed but not when channels are open (Flynn and Zagotta, 2001). This intersubunit disulfide bond might lock the cytoplasmic ends of two S6 helices in the closed configuration (Flynn and Zagotta, 2001). In the KcsA structure, the residues corresponding to S399C are close together (within 5–8 Å), whereas in MthK structure the residues are predicted to be far apart (separate by 20–30 Å). The closed and open conformations of CNGA1 channels therefore may be similar to KcsA and MthK, respectively.

Conclusions

By perturbing the S6 region through mutations and biochemical modifications, we have shown the importance of this region as part of the gating mechanism for CNG channels and gained some insights into the structure and rearrangement of the pore. We conclude that: (a) modification effects both gating and permeation, (b) the open configuration of the pore of CNGA1 channels is consistent with the structure of MthK, and

(c) the modification of the S6 disrupts the helical packing of the closed channel making it easier for the channels to open.

We would like to thank Drs. Matthew C. Trudeau, Jie Zheng, and Leon D. Islas for comments on this manuscript. We wish to thank Dr. Jos Van Schagen for helpful discussions and for computer algorithms that calculate coupled differential equations. We wish to acknowledge the members of the Zagotta lab who have contributed in many ways to the success of these experiments, especially the technical expertise of Kevin Black, Shellee Cunnington, Gay Sheridan, and Heidi Utsugi.

This work was funded by National Eye Institute (EY10329) and the Howard Hughes Medical Institute. W.N. Zagotta is an associate investigator within the Howard Hughes Medical Institute.

Olaf S. Andersen served as editor.

Submitted: 14 February 2003
Revised: 23 April 2003
Accepted: 2 May 2003

REFERENCES

Becchetti, A., K. Gamel, and V. Torre. 1999. Cyclic nucleotide-gated channels. Pore topology studied through the accessibility of reporter cysteines. *J. Gen. Physiol.* 114:377–392.

Becchetti, A., and P. Roncaglia. 2000. Cyclic nucleotide-gated channels: intra- and extracellular accessibility to Cd2+ of substituted cysteine residues within the P-loop. *Pflugers Arch.* 440:556–565.

Bucossi, G., M. Nizzari, and V. Torre. 1997. Single-channel properties of ionic channels gated by cyclic nucleotides. *Biophys. J.* 72: 1165–1181.

Burns, M.E., and D.A. Baylor. 2001. Activation, deactivation, and adaptation in vertebrate photoreceptor cells. *Annu. Rev. Neurosci.* 24:779–805.

Careaga, C.L., and J.J. Falke. 1992. Structure and dynamics of *Escherichia coli* chemosensory receptors. Engineered sulfhydryl studies. *Biophys. J.* 62:209–216.

Creighton, T.E. 1984. Disulfide bond formation in proteins. *Methods Enzymol.* 107:305–329.

Creighton, T.E. 1993. Proteins: structures and molecular properties, second edition. W.H. Freeman and Company, New York. 6 pp.

Doyle, D.A., J. Morais-Cabral, R.A. Pfuetzner, A. Kuo, J.M. Gulbis, S.L. Cohen, B.T. Chait, and R. MacKinnon. 1998. The structure of the potassium channel: molecular basis of K+ conduction and selectivity. *Science.* 280:69–77.

Enkvetchakul, D., G. Loussouarn, E. Makhina, S.L. Shyng, and C.G. Nichols. 2000. The kinetic and physical basis of K(ATP) channel gating: toward a unified molecular understanding. *Biophys. J.* 78: 2334–2348.

Espinosa, F., R. Fleischhauer, A. McMahon, and R.H. Joho. 2001. Dynamic interaction of S5 and S6 during voltage-controlled gating in a potassium channel. *J. Gen. Physiol.* 118:157–170.

Falke, J.J., A.F. Dernburg, D.A. Sternberg, N. Zalkin, D.L. Milligan, and D.E. Koshland, Jr. 1988. Structure of a bacterial sensory receptor. A site-directed sulfhydryl study. *J. Biol. Chem.* 263:14850–14858.

Fesenko, E.E., S.S. Kolesnikov, and A.L. Lyubarsky. 1985. Induction by cyclic GMP of cationic conductance in plasma membrane of retinal rod outer segment. *Nature.* 313:310–313.

Flynn, G.E., J.P. Johnson, Jr., and W.N. Zagotta. 2001. Cyclic nucleotide-gated channels: shedding light on the opening of a channel pore. *Nat. Rev. Neurosci.* 2:643–651.

Flynn, G.E., and W.N. Zagotta. 2001. Conformational changes in S6 coupled to the opening of cyclic nucleotide-gated channels. *Neuron.* 30:689–698.

Fodor, A.A., S.E. Gordon, and W.N. Zagotta. 1997. Mechanism of tetracaine block of cyclic nucleotide-gated channels. *J. Gen. Physiol.* 109:3–14.

Gordon, S.E., and W.N. Zagotta. 1995a. A histidine residue associated with the gate of the cyclic nucleotide-activated channels in rod photoreceptors. *Neuron.* 14:177–183.

Gordon, S.E., and W.N. Zagotta. 1995b. Subunit interactions in coordination of Ni^{2+} in cyclic nucleotide-gated channels. *Proc. Natl. Acad. Sci. USA.* 92:10222–10226.

Goulding, E.H., G.R. Tibbs, D. Liu, and S.A. Siegelbaum. 1993. Role of H5 domain in determining pore diameter and ion permeation through cyclic nucleotide-gated channels. *Nature.* 364: 61–64.

Guex, N., and M.C. Peitsch. 1997. SWISS-MODEL and the Swiss-PdbViewer: an environment for comparative protein modeling. *Electrophoresis.* 18:2714–2723.

Hackos, D.H., T.H. Chang, and K.J. Swartz. 2002. Scanning the intracellular S6 activation gate in the shaker K+ channel. *J. Gen. Physiol.* 119:521–532.

Hamill, O.P., A. Marty, E. Neher, B. Sakmann, and F.J. Sigworth. 1981. Improved patch-clamp techniques for high-resolution current recording from cells and cell-free membrane patches. *Pflugers Arch.* 391:85–100.

Heginbotham, L., Z. Lu, T. Abramson, and R. MacKinnon. 1994. Mutations in the K+ channel signature sequence. *Biophys. J.* 66: 1061–1067.

Henn, D.K., A. Baumann, and U.B. Kaupp. 1995. Probing the transmembrane topology of cyclic nucleotide-gated ion channels with a gene fusion approach. *Proc. Natl. Acad. Sci. USA.* 92:7425–7429.

Jan, L.Y., and Y.N. Jan. 1990. A superfamily of ion channels. *Nature.* 345:672.

Jiang, Y., A. Lee, J. Chen, M. Cadene, B.T. Chait, and R. MacKinnon. 2002a. Crystal structure and mechanism of a calcium-gated potassium channel. *Nature.* 417:515–522.

Jiang, Y., A. Lee, J. Chen, M. Cadene, B.T. Chait, and R. MacKinnon. 2002b. The open pore conformation of potassium channels. *Nature.* 417:523–526.

Jin, T., L. Peng, T. Mirshahi, T. Rohacs, K.W. Chan, R. Sanchez, and D.E. Logothetis. 2002. The (beta)gamma subunits of G proteins gate a K(+) channel by pivoted bending of a transmembrane segment. *Mol. Cell.* 10:469–481.

Johnson, J.P., Jr., and W.N. Zagotta. 2001. Rotational movement during cyclic nucleotide-gated channel opening. *Nature.* 412: 917–921.

Kaupp, U.B., T. Niidome, T. Tanabe, S. Terada, W. Bonigk, W. Stuhmer, N.J. Cook, K. Kangawa, H. Matsuo, T. Hirose, et al. 1989. Primary structure and functional expression from complementary DNA of the rod photoreceptor cyclic GMP-gated channel. *Nature.* 342:762–766.

Kramer, R.H., and E. Molokanova. 2001. Modulation of cyclic-nucleotide-gated channels and regulation of vertebrate phototransduction. *J. Exp. Biol.* 204:2921–2931.

Kraus-Friedmann, N. 2000. Cyclic nucleotide-gated channels in non-sensory organs. *Cell Calcium.* 27:127–138.

Lippiat, J.D., N.B. Standen, and N.W. Davies. 2000. A residue in the intracellular vestibule of the pore is critical for gating and permeation in Ca2+-activated K+ (BKCa) channels. *J. Physiol.* 529: 131–138.

Li-Smerin, Y., D.H. Hackos, and K.J. Swartz. 2000. A localized interaction surface for voltage-sensing domains on the pore domain of a K+ channel. *Neuron.* 25:411–423.

Liu, D.T., G.R. Tibbs, P. Paoletti, and S.A. Siegelbaum. 1998. Constraining ligand-binding site stoichiometry suggests that a cyclic-

nucleotide-gated channel is composed of two functional dimers. *Neuron*. 21:235–248.

Liu, D.T., G.R. Tibbs, and S.A. Siegelbaum. 1996. Subunit stoichiometry of cyclic nucleotide-gated channels and effects on subunit order on channel function. *Neuron*. 16:983–990.

Liu, J., and S.A. Siegelbaum. 2000. Change of pore helix conformational state upon opening of cyclic nucleotide-gated channels. *Neuron*. 28:899–909.

Loussouarn, G., E.N. Makhina, T. Rose, and C.G. Nichols. 2000. Structure and dynamics of the pore of inwardly rectifying K(ATP) channels. *J. Biol. Chem*. 275:1137–1144.

Loussouarn, G., L.R. Phillips, R. Masia, T. Rose, and C.G. Nichols. 2001. Flexibility of the Kir6.2 inward rectifier K(+) channel pore. *Proc. Natl. Acad. Sci. USA*. 98:4227–4232.

Lu, T., B. Nguyen, X. Zhang, and J. Yang. 1999. Architecture of a K+ channel inner pore revealed by stoichiometric covalent modification. *Neuron*. 22:571–580.

Lu, Z., A.M. Klem, and Y. Ramu. 2002. Coupling between voltage sensors and activation gate in voltage-gated K(+) channels. *J. Gen. Physiol*. 120:663–676.

Matulef, K., G.E. Flynn, and W.N. Zagotta. 1999. Molecular rearrangements in the ligand-binding domain of cyclic nucleotide-gated channels. *Neuron*. 24:443–452.

Matulef, K., and W. Zagotta. 2002. Multimerization of the ligand binding domains of cyclic nucleotide-gated channels. *Neuron*. 36: 93–103.

Minor, D.L., Jr., S.J. Masseling, Y.N. Jan, and L.Y. Jan. 1999. Transmembrane structure of an inwardly rectifying potassium channel. *Cell*. 96:879–891.

Molday, R.S., L.L. Molday, A. Dose, L.I. Clark, M. Illing, N.J. Cook, E. Eismann, and U.B. Kaupp. 1991. The cGMP-gated channel of the rod photoreceptor cell: characterization and orientation of the amino terminus. *J. Biol. Chem*. 266:21917–21922.

Molokanova, E., F. Maddox, C.W. Luetje, and R.H. Kram. 1999. Activity-dependent modulation of rod photoreceptor cyclic nucleotide-gated channels mediated by phosphorylation of a specific tyrosine residue. *J. Neurosci*. 19:4786–4795.

Nakamura, T., and G.H. Gold. 1987. A cyclic nucleotide-gated conductance in olfactory receptor cilia. *Nature*. 325:442–444.

Panchenko, V.A., C.R. Glasser, and M.L. Mayer. 2001. Structural similarities between glutamate receptor channels and K(+) channels examined by scanning mutagenesis. *J. Gen. Physiol*. 117: 345–360.

Roux, B., and R. MacKinnon. 1999. The cavity and pore helices in the KcsA K+ channel: electrostatic stabilization of monovalent cations. *Science*. 285:100–102.

Sadja, R., K. Smadja, N. Alagem, and E. Reuveny. 2001. Coupling Gβγ-dependent activation to channel opening via pore elements in inwardly rectifying potassium channels. *Neuron*. 29:669–680.

Shabb, J.B., and J.D. Corbin. 1992. Cyclic nucleotide-binding domains in proteins having diverse functions. *J. Biol. Chem*. 267: 5723–5726.

Shyng, S., T. Ferrigni, and C.G. Nichols. 1997. Control of rectification and gating of cloned KATP channels by the Kir6.2 subunit. *J. Gen. Physiol*. 110:141–153.

Stotz, S.C., and L.W. Haynes. 1996. Block of the cGMP-gated cation channel of catfish rod and cone photoreceptors by organic cations. *Biophys. J*. 71:3136–3147.

Sun, Z.P., M.H. Akabas, E.H. Goulding, A. Karlin, and S.A. Siegelbaum. 1996. Exposure of residues in the cyclic nucleotide-gated channel pore: P region structure and function in gating. *Neuron*. 16:141–149.

Sunderman, E.R., and W.N. Zagotta. 1999. Mechanism of allosteric modulation of rod cyclic nucleotide-gated channels. *J. Gen. Physiol*. 113:601–620.

Varnum, M.D., K.D. Black, and W.N. Zagotta. 1995. Molecular mechanism for ligand discrimination of cyclic nucleotide-gated channels. *Neuron*. 15:619–625.

Varnum, M.D., and W.N. Zagotta. 1996. Subunit interactions in the activation of cyclic nucleotide-gated channels. *Biophys. J*. 70: 2667–2679.

White, M.M., and M. Aylwin. 1990. Niflumic and flufenamic acids are potent reversible blockers of Ca2(+)-activated Cl^- channels in Xenopus oocytes. *Mol. Pharmacol*. 37:720–724.

Wohlfart, P., W. Haase, R.S. Molday, and N.J. Cook. 1992. Antibodies against synthetic peptides used to determine the topology and site of glycosylation of the cGMP-gated channel from bovine rod photoreceptors. *J. Biol. Chem*. 267:644–648.

Yau, K.W., and D.A. Baylor. 1989. Cyclic GMP-activated conductance of retinal photoreceptor cells. *Annu. Rev. Neurosci*. 12:289–327.

Yi, B.A., Y.F. Lin, Y.N. Jan, and L.Y. Jan. 2001a. Yeast screen for constitutively active mutant G protein-activated potassium channels. *Neuron*. 29:657–667.

Yi, B.A., D.L. Minor, Jr., Y.F. Lin, Y.N. Jan, and L.Y. Jan. 2001b. Controlling potassium channel activities: Interplay between the membrane and intracellular factors. *Proc. Natl. Acad. Sci. USA*. 98: 11016–11023.

Yifrach, O., and R. MacKinnon. 2002. Energetics of pore opening in a voltage-gated K(+) channel. *Cell*. 111:231–239.

Zagotta, W.N., T. Hoshi, and R.W. Aldrich. 1989. Gating of single Shaker potassium channels in *Drosophila* muscle and in Xenopus oocytes injected with Shaker mRNA. *Proc. Natl. Acad. Sci. USA*. 86: 7243–7247.

Zeidner, G., R. Sadja, and E. Reuveny. 2001. Redox-dependent gating of G protein-coupled inwardly rectifying K+ channels. *J. Biol. Chem*. 276:35564–35570.

Zhou, Y., J.H. Morais-Cabral, A. Kaufman, and R. MacKinnon. 2001. Chemistry of ion coordination and hydration revealed by a K+ channel-Fab complex at 2.0 A resolution. *Nature*. 414:43–48.

Zimmerman, A.L., J.W. Karpen, and D.A. Baylor. 1988. Hindered diffusion in excised membrane patches from retinal rod outer segments. *Biophys. J*. 54:351–355.

Zufall, F., and S.D. Munger. 2001. From odor and pheromone transduction to the organization of the sense of smell. *Trends Neurosci*. 24:191–193.